

Pro-inflammatory potential of different sizes of silica nanoparticles in bronchial epithelial lung cells (BEAS-2B)

Hang Le Thuy Pham



**Master thesis at
School of Pharmacy**

Department of Pharmaceutical Biosciences

Faculty of Mathematics and Natural Sciences

UNIVERSITY OF OSLO

2014

Pro-inflammatory potential of different sizes of silica nanoparticles in bronchial epithelial lung cells (BEAS-2B)

Master thesis in Pharmacy

Collaboration between



UiO : **School of Pharmacy**
University of Oslo

Department of Pharmaceutical Biosciences
School of Pharmacy
Faculty of Mathematics and Natural Sciences
University of Oslo

and



Department of Air Pollution and Noise
Division of Environmental Medicine
Norwegian institute of Public Health

Supervisors:
Tonje Skuland
Magne Refsnes
Marit Låg
Ragnhild Paulsen

© Hang Le Thuy Pham, 2014

Pro-inflammatory potential of different sizes of silica nanoparticles in bronchial epithelial lung cells (BEAS-2B)

<http://www.duo.uio.no/>

Print: Representeren, University of Oslo

Acknowledgements

To my supervisors. Thank you for your full support, guidance and motivation. I would not have come this far without your help. My deepest appreciation is particularly extended to Tonje. Thank you for always being there, for helping me with every aspects of my thesis and for sharing your experience and knowledge.

To the whole gang at MILS. Thank you for welcoming me with open arms when I first arrived. Your help and guidance concerning my laboratory work is very much appreciated. You have all been an inspiration. I will miss all the after-lunch cakes and the hallway- and office conversations.

To my family and friends. Thank you for your support and encouragement during this last year and particularly the last weeks of the thesis. Even though many of you do not understand what my thesis is about, your company and presence are were appreciated.

Hang Le Thuy Pham

Oslo, May 2014

Abstract

Nanotechnology is a growing industry with increased use of nanomaterials in several fields, such as medicine, cosmetics and food products. Nanoparticles are defined as particles of 1 to 100 nanometers size in two or three dimensions. The small size gives rise to a large surface-to-mass ratio compared to the bulk of the same material, which increases as the particle size reduces. Their unique properties and increased use actualize the need to characterize their biological and potentially hazard effects. The biological effects of nanoparticles are closely related to their physicochemical properties, such as particle size, particle charge, agglomeration state and surface chemistry. It has previously been shown that non-crystalline (amorphous) silica nanoparticle (SiNP) of 50 nm inherits pro-inflammatory potentials by inducing the release of several cytokines, including IL-6 and IL-8. In the present study, the pro-inflammatory and cytotoxic potentials of three different sizes of silica nanoparticles, 10 nm (Si10), 12 nm (Si12) and 50 m (Si50) in bronchial epithelial cells (BEAS-2B) were characterized. The involvement of the signalling mechanisms MAPKs p38, JNK and ERK and TGF- α /EGFR-pathways, in mediating the release of the cytokines IL-6, IL-8 and RANTES, were further studied by exposing BEAS-2B cells to Si10 and Si50. In addition, characterization of particle size and particle charge of the respective SiNPs was performed with dynamic light scattering (DLS) in the exposure cell culture medium.

The study showed a concentration-dependent release of IL-6, IL-8, RANTES and lactate dehydrogenase (LDH) 20 hours after Si10, Si12 and Si50 exposure in BEAS-2B cells. There was a particular large difference between the ability of Si10 and SI12 to induce cytokine release with respect to the small size difference. This was not seen for the LDH release. Si10 induced highest levels of IL-6 and IL-8, followed by Si12 and Si50. A similar release pattern was shown for RANTES; however, the Si12 responses were more like the Si50 responses. The particle characterization indicated the presence of large agglomerates in the Si10 and Si12 particle solution in DMEM/F-12 cell medium. The involvement of MAPKs in the cytokine release was further assessed by incubating BEAS-2B cells with chemical inhibitors and by studying the phosphorylation patterns of the signalling proteins. It was shown that p38 and JNK was involved in the release of IL-6 and IL-8 in Si10- and Si50-exposed cells. The RANTES release might be mediated by p38 and JNK, but also ERK. It was in addition

demonstrated the involvement of EGFR pathway in Si10- and Si50-induced cytokine release. The SiNP-induced release of the EGFR-ligand TGF- α was also demonstrated.

In conclusion, SiNPs induced a concentration-dependent cytokine release with order of potency Si10>>Si12>Si50 for IL-6 and IL-8 and Si10>>Si12=Si50 for RANTES. In addition, LDH release was concentration-dependent with the order of potency Si10>Si12>>Si50. Si10 and Si50 activated the same signalling mechanisms, and the SiNP-induced cytokine releases seem to partly involve MAPK p38 and JNK and EGFR-pathway. TGF- α might be involved in Si10- and Si50-induced cytokine release through EGFR. However, the role of TGF- α was unclear, and needs to be clarified further. Particle characterization of Si10, Si12 and Si50 indicated that other parameters in addition to particle size might be important for the pro-inflammatory and cytotoxic responses of SiNPs.

Abbreviations

BSA	Bovine serum albumin
EGF	Epidermal growth factor
ADAM	A disintegrin and metalloproteinase
AP-1	Activator protein 1
C/EBP	CCAAT-enhancer-binding proteins
CXCL8	See IL-8
DLS	Dynamic light scattering
EGFR	Epidermal growth factor receptor
ELISA	Enzyme-linked immunosorbent assay
ELS	Electrophoretic light scattering
ERK	Extracellular signal-regulated kinases
IL-1	Interleukin-1
IL-6	Interleukin-6
IL-8	Interleukin-8
JNK	c-JUN N-terminal kinase
LDH	Lactate dehydrogenase
MAP2K	See MAPKK
MAP3K	See MAPKKK
MAPK	Mitogen-activated protein kinase
MAPKAP	MAPK-activated protein kinase
MAPKK	Mitogen-activated protein kinase kinase
MAPKKK	Mitogen-activated protein kinase kinase kinase
MEK	See MAPKK
MK	MAPKAP kinase
MKK	See MAPKK
NF- κ B	Nuclear factor kappa-light-chain-enhancer of activated B cells
PBS	Phosphate buffered saline
Ser	Serine
Si10	Silica nanoparticle 10 nm
Si12	Silica nanoparticles 12 nm
Si50	Silica nanoparticle 50 nm
siNP	Silica nanoparticle
STAT	Signal transducer and activator of transcription
TEM	Transmission electron microscopy
TGF- α	Transforming growth factor- α
Thr	Threonine
TNF- α	Tumor necrosis factor- α

Table of contents

Abstract	VI
Abbreviations	VIII
Table of figures	XII
1 Introduction	1
1.1 Properties of nanoparticles	2
1.1.1 Two distinctive properties of nanomaterials.....	2
1.1.2 Physicochemical properties of colloid suspension.....	3
1.1.2.1 Kinetic properties.....	3
1.1.2.2 Agglomeration	4
1.1.2.3 Surface charge.....	5
1.1.2.4 Protein corona	6
1.1.2.5 Interparticular forces	8
1.1.3 The importance of dispersion of nanoparticles	8
1.2 The respiratory system	9
1.2.1 The architecture.....	9
1.2.2 Cells in the trachea-bronchial region and mucus.....	9
1.2.3 Cells in the alveolar region.....	11
1.3 Particle deposition in the airways	11
1.3.1 Mechanisms of particle deposition.....	11
1.3.1.1 Inertial impaction and gravitational forces	12
1.3.1.2 Brownian diffusion	12
1.3.2 Physiological factors affecting particle deposition.....	13
1.3.3 Defence mechanisms in the airways.....	13
1.3.3.1 Mucociliary clearance.....	13
1.3.3.2 Alveolar macrophages.....	14
1.3.4 Factors involved in local versus systemic effect.....	14
1.3.4.1 Systemic absorption of inhaled nanoparticles	15
1.4 Inflammation	15
1.4.1 Pro-inflammatory cytokines.....	16
1.4.2 Acute and chronic inflammation	17
1.4.3 Inflammation in the lungs.....	18
1.4.3.1 Pulmonary fibrosis	18
1.5 Intracellular signalling pathways	19
1.5.1 Mitogen-activated protein kinase signalling pathways.....	19
1.5.2 Epidermal growth factor receptor (EGFR).....	23
1.5.2.1 Transforming growth factor (TGF)- α	24
1.5.3 Interplay between signalling pathways	25
1.5.4 IL-8 in light of the signalling pathways.....	27
1.6 Silica particles and inflammatory responses	28
2 Aims of the study	31

3	Material and methods	32
3.1	Materials	32
3.1.1	Silica nanoparticles	32
3.1.2	Other materials used in the study	32
3.1.3	Solutions used in the study	32
3.1.4	Cell line and cell culture medium	33
3.2	Methods: The principles	34
3.2.1	Particle characterization with light scattering	34
3.2.1.1	Determination of particle size and polydispersity with dynamic light scattering	34
3.2.1.2	Determination of particle zeta potential with electrophoretic light scattering	35
3.2.2	Western blotting	36
3.2.2.1	Cell lysis and sample preparation	36
3.2.2.2	Gel electrophoresis	36
3.2.2.3	Immunoblotting	37
3.2.2.4	Immunodetection	37
3.2.3	Enzyme-linked immunosorbent assay (ELISA)	38
3.2.4	Small interfering RNA (siRNA)	40
3.2.5	Colorimetric lactate dehydrogenase (LDH) assay	41
3.3	Methods: Procedures	42
3.3.1	Preparing the particle solutions	42
3.3.2	Cell growth	42
3.3.3	Particle characterization	42
3.3.4	Silica nanoparticle exposure to BEAS-2B cells	43
3.3.5	The use of chemical inhibitors	44
3.3.6	The use of siRNA	44
3.3.7	Analysis of TGF- α release	44
3.3.8	Sample preparation and procedures for analysis with ELISA and LDH assay	45
3.3.8.1	Sandwich ELISA	45
3.3.8.2	The LDH assay	45
3.3.9	Western analysis	46
3.4	Statistical considerations	47
3.5	Methodological considerations	48
3.5.1	Theoretic particle number in 2 mg/ml Si10 and Si50 particle solution	48
3.5.2	Theoretical surface area of 25 μ g/ml Si10 and 200 μ g/ml Si50 exposed to the cells	48
3.5.3	Particle characterization of Si10 particle solution with DLS	49
3.5.4	The preparation of particle solution – is it optimal?	49
3.5.5	The stability of a new and old Si10 particle solution	52
3.5.6	Consideration of cell medium	52
4	Results	53
4.1	Characterization of size and charge of silica nanoparticles	53
4.2	The release of cytokines	56
4.3	Cytotoxicity	58
4.4	Involvement of intracellular signalling pathways in the cytokine release	59

4.4.1	Involvement of MAPKs pathways in cytokine release	59
4.4.1.1	Activation of MAPKs after exposure to Si10 and Si50	59
4.4.1.2	The involvement of MAPKs in cytokine release	63
4.4.2	The involvement of TGF- α /EGFR pathway on the cytokine release.....	65
4.4.2.1	Inhibition of EGFR and TACE.....	66
4.4.2.2	Release of TGF- α	67
5	Discussion	68
5.1	Particle characterization.....	68
5.2	Cytokine and LDH release related to particle properties	70
5.2.1	Particle size – is it really the determinant factor?.....	71
5.3	Signalling pathways involved in the cytokine release	74
5.4	<i>In vivo</i> extrapolation	78
6	Conclusions.....	79
7	References	80
	Appendix 1: Other materials used in the study.....	86
	Appendix 2: Solutions used in the study	91
	Appendix 3: Particle characterization of 100 μg/ml Si10, Si12 and Si50 in water	95

Table of figures

Figure 1: The scale of objects.....	2
Figure 2: Agglomeration of particle solution.....	4
Figure 3: Diagram of particle surface with subsequent surface potential (zeta potential).....	6
Figure 4: Simplified illustration of different proteins adsorbing to particle surface with different kinetics.....	8
Figure 5: The respiratory tract.....	10
Figure 6: Simplified illustration of ciliated cells with mucus.....	10
Figure 7: Particle deposition mechanisms of importance.....	12
Figure 8: Simplified illustration of the three-tiered MAPKs signalling pathway.....	21
Figure 9: Principle of sandwich ELISA.....	40
Figure 10: Principle of LDH assay.....	41
Figure 11. Comparison between one week old and newly made particle solution of Si1.....	52
Figure 12. The size distributions and particle charge of 100 µg/ml of Si10, Si12 and Si50....	54
Figure 13. Release of IL-6, IL-8 and RANTES after exposure to Si10, Si12 and Si50 in BEAS-2B cells.....	57
Figure 14. The release of LDH after exposure to Si10, Si12 and Si50 in BEAS-2B cells.....	58
Figure 15A. Western blotting of phosphorylated MAPK after exposure to Si10 and Si50.....	60
Figure 15B. Western blotting of phosphorylated MAPK after exposure to Si10 and Si50.....	61
Figure 16. Dose-dependent phosphorylation of p38, ERK and JNK.....	62
Figure 17. The involvement of MAPKs in cytokine release after exposure to Si10 and Si50.....	64
Figure 18. Effect of siRNA against JNK on cytokine release induced by Si10 and Si50.....	65
Figure 19. The involvement of EGFR and TACE in cytokine release after exposure to Si10 and Si50.....	66
Figure 20. TGF-α release after exposure to Si10 and Si50.....	67

1 Introduction

Nanoparticles are airborne, naturally occurring materials. Humans have therefore always been exposed to nanoparticles since the existence of life. But anthropogenic sources have increased the number of nanoparticles in air pollution drastically in the later years [1]. Humans can therefore come in contact with nanoparticles through air pollution and occupational exposure [2-5]. Inhaled nanoparticles can translocate to the systemic circulation, exposing other vital organs and systems [6]. This raises concerns from a public health perspective. But in addition, the nanoparticles inherit particular interesting properties, making them very useful in many fields, including the pharmaceutical industry. Nanoparticles can be used in formulation or as parts of drugs, but also as diagnostic and imaging agents [6, 7]. Even though the latter is very helpful for both the society and patients, safety assessments are still needed before sick and weakened humans are exposed to potentially harmful nanoparticles. It is very central in pharmaceutical productions to establish a risk-benefit analysis for a particular product. The quality of this analysis is not high if the knowledge of the toxicity profile of the nanomaterials used is limited.

Nanomaterials are also found in many different products, such as cosmetics, electronics and plastics [6, 8]. The increasing use of nanoparticles is due to their unique properties, but is also the reason why there is a great need to study and characterize their toxicity. Their unusual properties may make existing tests and procedures inadequate in detecting their hazard effects. Additional assays are needed, but this requires increased understanding of the nanoparticles' properties and effects [9]. The agglomeration of nanoparticles further complicates the issues, as coarse agglomerates have been shown to exert different biological effects compared to monodispersed nanoparticles [6]. The characterization of the particles' physical properties is therefore also an important step in understanding their toxic potential.

1.1 Properties of nanoparticles

Nanoparticles are widely defined as particles where two or three of the dimensions range from 1 to 100 nanometers [6, 7]. This is in the size range of molecules, proteins and small viruses (figure 1) [10, 11]. They occur in many different geometric shapes, and can be of biological or non-biological origin (engineered nanoparticles) [9].

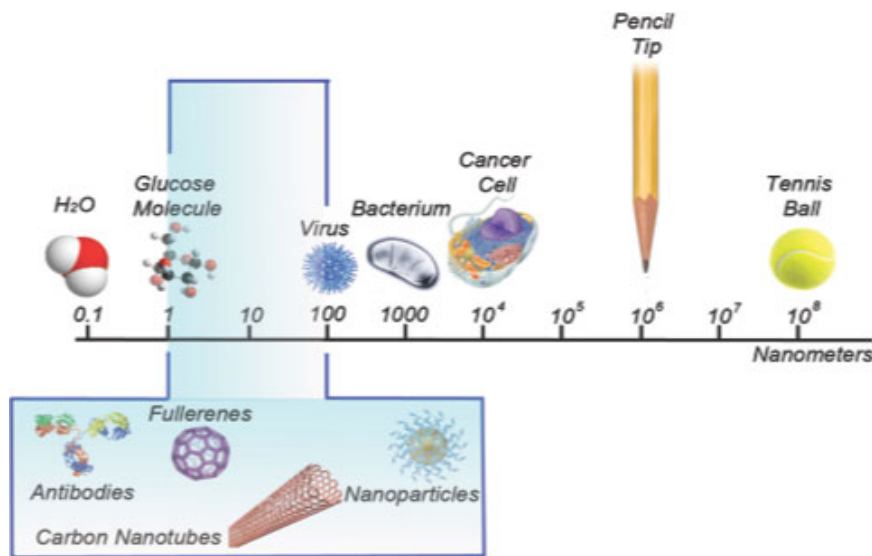


Figure 1: The scale of objects.

<http://inl.int/what-is-nanotechnology-2>

1.1.1 Two distinctive properties of nanomaterials

Most of the large interest in nanomaterials can be awarded to two special properties. Nanomaterials inherit a set of quantum properties due to a different electron distribution, which gives the materials special electrical-, magnetic- and optic properties. These effects are of lesser importance for biological effects, but are, however, of special interest in other areas [12, 13].

Another special feature of nanoparticles is their small particle size, giving a surface-to-mass (or surface-to-volume) ratio that is larger than their respective bulk material. This ratio increases as the particle size is reduced, and they have therefore a large surface area compared to mass or volume. Consequently, there are also many more atoms on the surface per mass unit. This property represents one of the reasons why nanoparticles are so interesting [9, 12], and it is thought that increased surface area (but also their surface properties) gives increased toxicity as well as reactivity [9]. This indicates that smaller particles exert different biological- and toxic effects than larger particles. With the increased number of atoms per mass unit, the surface of the nanoparticles can be manipulated with different molecules, making it an interesting tool, also for drug delivery [9, 14].

The biological effects of nanoparticles are related to their physicochemical properties, such as particle size, particle shape, agglomeration state and surface chemistry. Therefore there has been increasingly focus on appropriate characterization of particle properties [8, 15]. In studies, this characterization is equally important when assessing biological effect because it ensures correct and reproducible results [8].

1.1.2 Physicochemical properties of colloid suspension

A suspension is a system where particles, the disperse phase, are dispersed throughout a liquid, the continuous phase. Nanoparticles dispersed in a liquid are often referred to as a *colloid* suspension. The term colloid is referred to when the dispersed particles are within the size range of 1-1000 nm, including the range of nanoparticles [16].

1.1.2.1 Kinetic properties

The movement of colloidal particles in suspension is a result of thermal motion in form of Brownian motion and diffusion. Brownian motion is due to the random collisions between the particles of the disperse phase and the molecules of the continuous phase. The consequence is a random and irregular particle movement. Brownian motion also allows the particles to

move, i.e. diffuse, from a region of high concentration to one of lower concentration. Both these processes are affected by size, and the determination of diffusion coefficient through dynamic light scattering (see section 3.2.1.1) can be used to determine particle size. These processes are affected by particle size, viscosity of the continuous phase and temperature, i.e. there is increased movement with increased temperature, and reduced movement with increased liquid viscosity and particle size [16, 17]. It is also thought that the particles can move because of convection forces due to density fluctuations in suspensions [13].

1.1.2.2 Agglomeration

Because of the small size of nanoparticles, the particles have a high surface tension. To reduce the tension, the particles tend to agglomerate producing larger particles (figure 2) [16]. The surface chemistry, i.e. hydrophobicity, hydrophilicity and ionization, will affect the presence of attractive and repulsive forces and thereby the interactions between particles [17].

The particles in this kind of agglomerate are normally bound together through attractive forces. Other factors contributing to agglomeration are particle concentration and surface properties. With increasing concentration, the number of particles is increased; the particles lie more closely together, as well as increasing the chances for particle collision. A suspension of monodispersed particles can therefore agglomerate to make larger particle masses, which are more prone to sedimentation, and give rise to polydispersity, where the dispersion consists of particles of different sizes.

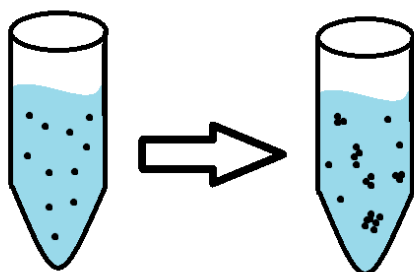


Figure 2: Agglomeration of particle solution.

1.1.2.3 Surface charge

The surface charge of particles influences whether the particles will be separately dispersed or agglomerate. There are several mechanisms where the particle surface can acquire charge, i.e. ion dissolution, ionization and ion adsorption. The surface can have both positive and negative charge, but it is the net charge that defines the electrical potential of the surface. Ion dissolution is based on the surface groups being salts and the charge are acquired due to unequal dissolution of oppositely charged molecules. The surface potential is then determined by which ion is in excess. In ionization, the surface has ionisable chemical molecules that ionize depending on pH of the solution. Ion adsorption, on the other hand, is based on specific adsorption of charged ions to the surface affecting the net surface charge [16].

In particle research, zeta potential is used to determine surface charge (figure 3). Normally, in an aqueous solution with particles, there are both negative and positive ions present. The surface charge of the particles will affect the distribution of these ions, because ions of opposite charge (counter-ions) will, non-specifically, be attracted to the surface whereas ions of same charge (co-ions) will be repelled. Some ions of the same charge will, although, also be present close to the surface due to the need for an electrically neutral system. The particle surface and the ions together make up the electrical double layer.

The electrical double layer consists of an inner layer, which includes particle surface and potentially specific adsorbed ions, and a diffuse layer where the ions are diffusely distributed based on electrostatic forces and thermal motion. A Stern plane separates these two layers, which is a sheet of counter-ions that are attracted through electrostatic forces based on the charge of the inner layer (surface charge). The diffuse layer of both positive and negative ions reaches from the Stern plane and outwards. Depending on the charge of the inner layer, the concentration of the counter-ions will decrease with increasing distance from the surface, and the concentration of co-ions will increase with increasing distance, until they reach an equal concentration, whereas the potential becomes zero and the system is electrical neutral.

A little further out of the Stern plane, is the Shear or slipping plane. This is the surface of a solvating layer, a layer that is made by the binding of solvent to the particle surface and adsorbed ions. The particle with its solvating layer is defined as the effective surface, in which the solvating layer moves together with a particle in motion. The Shear plane therefore represents the border of movement between inner layer and the continuous phase. The potential at the Shear plane is referred to as zeta potential, which represents the particle surface charge dispersed in suspension rather than the true surface charge [16, 18]. A zeta potential higher than 30 mV or lower than -30 mV is assumed to give a stable suspension with monodispersed particles [6].

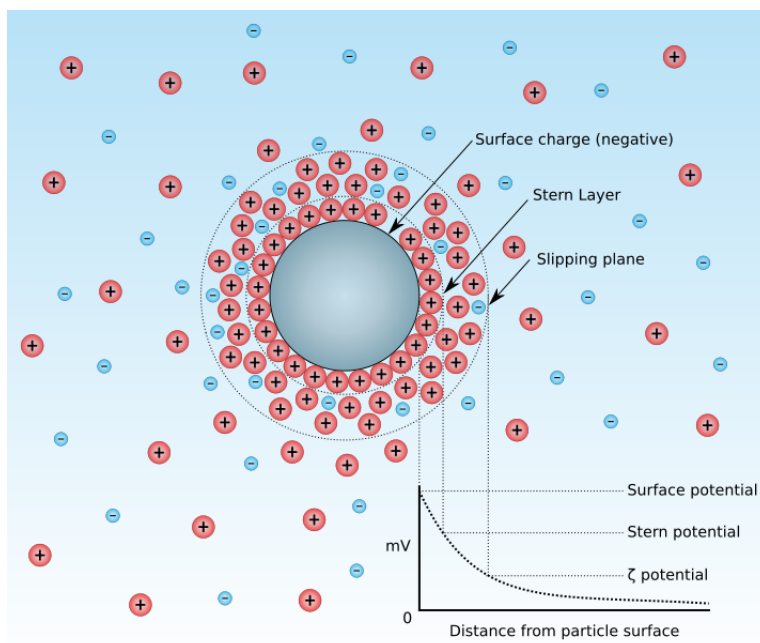


Figure 3: Diagram of particle surface with subsequent surface potential (zeta potential).

http://en.wikipedia.org/wiki/Zeta_potential

1.1.2.4 Protein corona

Upon contact with biological medium, proteins cover nanoparticles, promoting the formation of a protein corona covering the particle surface (figure 4) [19, 20]. This has multiple effects on the nanoparticle; increased particle size, modified surface, modified particle-particle- and particle-cell interactions. This again influences the particles' physical stability and the

biological effects exerted by them. Moreover, some proteins undergo conformational changes upon adsorption, which may disturb these proteins' biological functions [20-22].

The composition of the protein corona is thereby of particular importance. In an environment rich of biomolecules, the composition of the protein corona is dependent on physicochemical properties of the nanoparticles, the environment, duration of exposure and competition between different proteins. The total amount of proteins adsorbed is roughly constant, but the composition may alter over time [21].

The protein corona is multi-layered and can be divided into hard- and soft corona. Proteins that form the hard corona bind the surface with high affinity and desorb to a low extent. The hard corona is thereby a stable layer with little dynamic. The soft corona is made of low-affinity proteins that are more loosely bound to the surface. These proteins desorb easily and are subject to competition from other proteins. It is thought that proteins of the soft corona are bound, through protein-protein interactions, with proteins of the hard corona. It is assumed that each protein has its own association- and dissociation rates, which explains the adsorption and desorption of proteins. Due to the stability of the hard corona, it is this protein layer, along with the particle, that is believed to be the biological identity of a nanoparticle [19, 21]. There has also been demonstrated that biological medium and temperature influences the formation and composition of the protein corona, which thereby affects the cellular interactions and the following effects [23, 24].

Due to the dependence of the protein corona on physicochemical properties of nanoparticles, difference in size among nanoparticles of same materials is also thought to give different protein corona. The nanoparticles affect the protein corona mainly through their surface charge and hydrophobicity [19]. Research shows a tendency for hydrophobic or charged particles to adsorb and denature more proteins than neutral or hydrophilic particles [21]. It is also believed that increased surface area, i.e. smaller particles, adsorb more proteins [19].

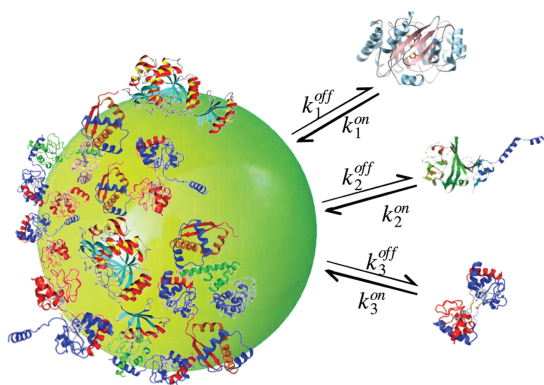


Figure 4: Simplified illustration of different proteins adsorbing to particle surface with different kinetics.

http://figshare.com/articles/_Schematic_of_nanoparticle_protein_corona_formation_process_/710422

1.1.2.5 Interparticular forces

There are mainly two types of forces between particles; repulsive and attractive. The attractive, van der Waals forces pull the particles together, promoting agglomeration. Repulsive, electrostatic forces, on the other hand, push the particles further apart. Whether the particles agglomerate or not depends on the net force; agglomeration is avoided when the total repulsive forces are larger than the total attractive forces. The range of the repulsive forces depends on the thickness of the electrical double layer, and arises from the interaction between the particles' electrical double layers. Another way to avoid particle agglomeration is through steric forces. By adhering macromolecules specifically to the particle surface, the particles cannot come in contact with each other, and thereby cannot agglomerate [18].

1.1.3 The importance of dispersion of nanoparticles

The physical stability of a suspension is affected by additives such as proteins and electrolytes. The size of the nanoparticles is an important factor of their effect as well as toxicity. It is therefore necessary to make particle solutions that will maintain the individual particles, i.e. monodispersed. But in *in vitro* research with cells, nanoparticles are normally dispersed in aqueous solutions with physiological pH and salt concentrations to mimic

physiological conditions. And as described earlier, this promotes unwanted particle agglomeration, which has also been confirmed by several studies [6, 25-27]. Since monodispersity often is of preference, it is important to have an optimum method for dispersing the nanoparticles. Studies have shown that ultra-sonication followed with the addition of a stabilizer gives stable suspensions. The sonication will deagglomerate agglomerated particles, whereas the stabilizer will adsorb to the particle surface, making it steric impossible for individual particles to agglomerate. The stabilizer will although increase particle size due to its adsorption. Many substances can be used as stabilizers, ranging from serum, surfactants, polymers and proteins [6, 26, 28].

1.2 The respiratory system

1.2.1 The architecture

The respiratory tract starts at the nose and ends in the alveoli in the lungs (figure 5). It can roughly be divided into two parts - upper and lower respiratory tract – separated by the larynx. The lower respiratory tract is further divided in conducting airways and pulmonary airways. It starts from the larynx, continuing down the trachea, branching in two bronchi, one in each lung, which divides further to numerous bronchioles and end with millions of alveolar sacs in the lung walls. The branching follows a very irregular pattern. As the branching continues downwards, a reduction of tubules diameter and an increase in surface area take place. Each sac contains about 20 alveoli, tightly packed together separated by a common septum [29].

1.2.2 Cells in the trachea-bronchial region and mucus

The airway contains more than 40 different types of cells. The bronchi are lined with mainly ciliated and goblet cells together with a mucus layer. Other cells are serous cells, bush cells and Clara cells. The number of goblet cells and serous cells decreases downward the airways, whereas the number of Clara cells increases. Ciliated cells exist numerously from larynx to

the terminal bronchioles, covering the whole surface of this region, though the number decreases downwards. They are epithelial cells with hair-like extrusions (“cilia”) pointing inwards the airway lumen (figure 6). The cilia lie in an epithelial lining fluid produced by serous cells, but the tips project into a mucus layer. The cilia push the mucus upward to the throat through teamwork between the individual cilia [29].

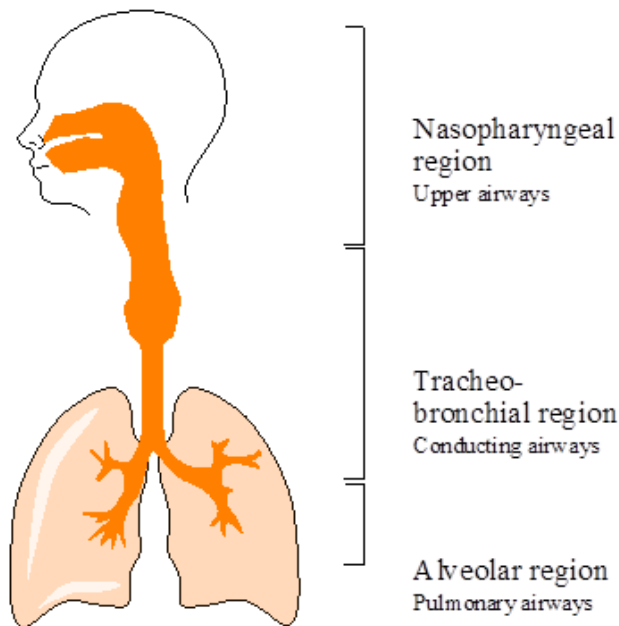


Figure 5: The respiratory tract.

The mucus layer is a viscoelastic layer which is produced mainly by the submucosal glands, but also some from the goblet cells. It consists of a mixture of glycoproteins, proteins and lipids [29].

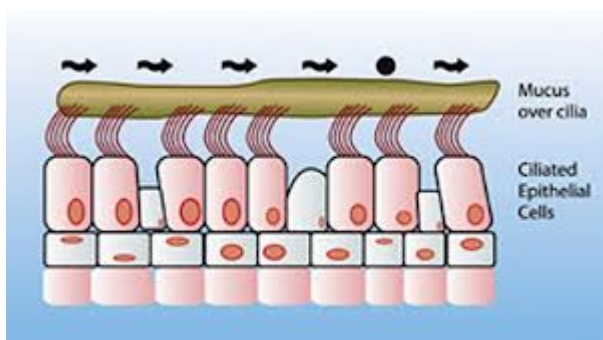


Figure 6: Simplified illustration of ciliated cells with mucus.

<http://biology-igcse.weebly.com/functions.html>

1.2.3 Cells in the alveolar region

In the alveolar region, there are no ciliated cells and mucus, but presence of alveolar macrophages. The epithelial cells here are very flat, divided into two: type 1 pneumocytes and type 2 pneumocytes. The surfaces of the alveolar sacs are mainly occupied by the type 1 cells. They are responsible for the diffusion between the airways and blood, and are therefore thin cells enabling a short airway-to-blood pathway. Type 2 cells produce pulmonary surfactant. It is a lipoprotein which function is to reduce the surface tension of the interface between alveoli and alveoli fluid, maintaining the architecture of the alveoli with their large surface area, and thereby enabling effective gas exchange. The type 2 cells are precursors of type 1 cells. Between the capillaries and the alveoli lies the interstitial space consisting of fibroblasts, macrophages and lymphocytes [29].

1.3 Particle deposition in the airways

There are many factors affecting the fate of an inhaled particle:

1.3.1 Mechanisms of particle deposition

Deposition depends on breathing pattern; deep breaths and breath holding increases deposition. And, of course, due to the increased narrowing of the airway, particle size also decides how far down the particles reach. Particles originally very small can be subject to agglomeration due to the moist environment in the airway [18]. Generally, the smaller the particles, the deeper penetration [30]. However, small nanoparticles less than 10 nm will deposit in the nasal area.

There are several deposition mechanisms in the airways [18, 29]. Inertial impaction, Brownian diffusion and gravitational settling are among the most important (figure 7) [29]. The dominant mechanism depends on particle size. Particles over 3 μm are subject to impaction, particles over 0.5 μm are subject to gravitational settling and particles under 0.5 μm are subject to Brownian motion [31].

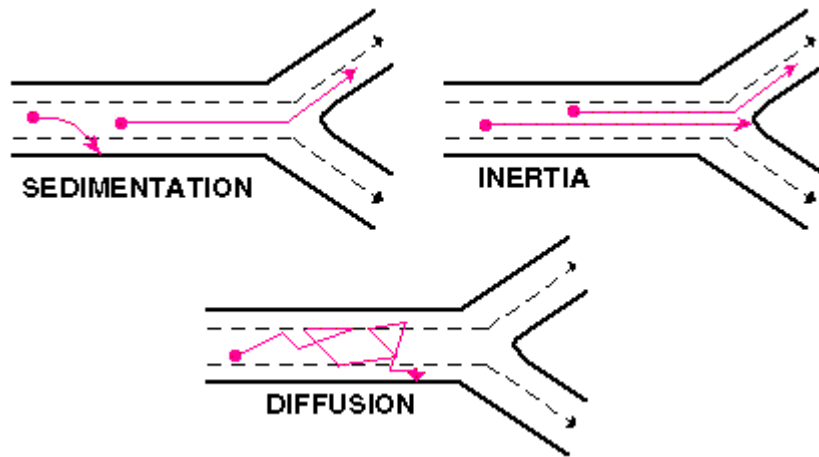


Figure 7: Particle deposition mechanisms of importance.

<http://www.coheadquarters.com/PennLibr/MyPhysiology/lect6p/lect6.02.htm>

1.3.1.1 Inertial impaction and gravitational forces

Large and heavy particles are subject to inertial forces early in the airways. Due to their slow movement, they are not able to follow the changes in the airflow in the airways. These particles will therefore most likely collide and deposit in the airways surface around the trachea where branching of the respiratory tract starts. In the narrower, branched airways, the particles deposit mainly due to gravitation forces [18].

1.3.1.2 Brownian diffusion

Very fine particles, i.e. light particles, are subject to diffusion and can deposit everywhere in the airway. Small particles that reach far down the airways can deposit here due to the little airflow velocity. It is assumed that the cut-off is about $0.5 \mu\text{m}$ for particles to reach the alveoli [18]. Although these particles are able to reach far down the lungs, their small size also makes them vulnerable for exhalation with the air. Only very small particles, roughly 100 nm and down, are so small that they have large thermic motion, enabling them to collide with the airways before exhalation [31]. The smaller the particle, the larger is the possibility for diffusional settling [29].

1.3.2 Physiological factors affecting particle deposition

Breathing through the nose increases the probability for particle deposition in the nose and pharynx. For a particle to reach the alveoli, it needs to be mainly breathed through the mouth. It also needs to stay in the airflow, away from any contact with the surface at all times, and be able to change directions accordingly. The increasing branching of the respiratory tract with reduced lumen diameter and length present the particles with a huge challenge [29].

The pattern of deposition is depended on the method of breathing. Deposition (by impaction) is enhanced in the pharynx and larynx with increased inspiratory flow rate due to the increased particle momentum and turbulence that follows. Breath holding, in the other hand, increases the time for gravitational settling to occur. Increased tidal volume (“deep breath”) increases the chances of deep penetration [29].

It is also important to remember that anatomical and physiological alternations due to, for instance diseases, will influence particle deposition [29].

1.3.3 Defence mechanisms in the airways

Deposited particles can still be cleared from the airways through two important defence mechanisms in the airways:

1.3.3.1 Mucociliary clearance

The ciliated epithelial cells, reaching from about the terminal bronchioles to the trachea, function to propel mucus upwards towards the throat to be swallowed. In this defence mechanism, entrapped particles in the mucus are eliminated from the airways. It takes a few hours for deposited particles to be eliminated through this method. The efficiency of the mucociliary clearance is highly dependent on the viscosity and thickness of the mucus [29]. It

is also thought that surfactants can bind to hydrophobic particles, thereby increase the particles displacement in the mucus and facilitate clearance by macrophages [30].

1.3.3.2 Alveolar macrophages

In the alveolar region, there are macrophages that can engulf particles, rapidly removing them. The macrophages can then either transport the particles to the mucociliary clearance system or be transported via the lymphatic systems to the blood stream. This clearance mechanism takes up to days or weeks [29].

1.3.4 Factors involved in local versus systemic effect

Whether a particle is absorbed locally or systemically depends on several factors. First of all, the particle cannot exert local effect if it is rapidly cleared either by the cilia or the macrophages. For the particle to be absorbed to the systemic circulation, the anatomy of the airways is of particular importance. Systemic absorption through the alveoli is the greatest due to their large surface area, thin membrane and rich blood supply [29].

The main absorption barrier in the airways lies with the epithelium in the lung wall, though the epithelium of the lung is much more permeable than of other routes. There are tight junctions between type 1 pneumocytes with a gap of about 1 nm, but there exist about 10 nm pores, too. As with all other membranes, systemic absorption can be done paracellular or transcellular; lipophilic compounds transcellularly and hydrophilic compounds paracellularly, respectively. The particular large junctions between the cells enable a higher degree of paracellular absorption compared to other routes. Active, transcellular transport in form of endocytosis or carrier-mediated transport can also take place [29].

1.3.4.1 Systemic absorption of inhaled nanoparticles

The pulmonary health risks associated with inhalation of particulate matter, for instance pollution, were briefly described above. In addition to possible locally diseases (pulmonary), inhalation of particulate pollution has been shown to increase morbidity and mortality through cardiovascular diseases (extrapulmonary effects). The mechanisms responsible for these effects are yet unclear, but several hypotheses have been suggested, including systemic release of inflammatory mediators affecting the cardiovascular system [32], particulate pollution affecting the autonomic nervous system controlling the heart (“respiratory reflexes”) [33] and translocation of particles from lungs to the systemic circulation. An interest has been on the latter, many studies showing a systemic absorption of inhaled nanoparticles in both animals and humans [34-36]. However, other studies show that most of the nanoparticles might be maintained in the lung tissue. In spite of this, much attention and concern have been raised whether nanoparticles can potentially migrate to any organ and exert their negative effects.

1.4 Inflammation

Inflammation is a protective response against a harmful substance or process, leading to activation of multiple cell types with release of inflammatory proteins and mediators. The inflammatory process is induced by the release of pro-inflammatory cytokines and mediators from damaged cells. The goals are to eliminate the cause, remove the subsequent dead cells and repair damage. This is done by the infiltration of inflammatory components to the affected tissue. Since the components of the inflammatory process are programmed to attack and kill foreigners, they will also harm innocent, neighbouring host cells. During inflammation in a given tissue, the local blood capillaries dilate, the permeability increases and the rate of the blood flow reduces. This promotes the movement of body fluid, plasma proteins and leukocytes into the tissue, leading to the characteristic symptoms of pain, heat, swelling and reddening.

1.4.1 Pro-inflammatory cytokines

Cytokines are a group of secreted proteins central for the inflammatory process. They are therefore often referred to as pro-inflammatory cytokines. They regulate many processes, particularly the immune- and inflammatory responses. The cytokines exert their effect through binding on surface receptors and activate a diverse range of target cells, changing their pattern of gene expression. There are many types of cytokines, each with a different function, and are produced and released from different cell types due to an external stimulus. One cytokine can for example stimulate a target cell to transcribe and produce another type of cytokine, which again activate another cell type to produce another cytokine, and so on, creating a massive inflammation involving different cell types and inflammatory mediators. Cytokines can, depending on the type, also exert both local and systemic effects.

Interleukin-6 (IL-6) is a cytokine that regulates acute-phase immune response [37]. It has mainly systemic effects, inducing fever and stimulating the production of acute-phase proteins by hepatocytes in the liver. The acute-phase proteins bind to the surface of microorganisms, acting as opsonins and activator of complement system. It is also an activator of the adaptive immune system. IL-6 is released by several cell types, and is synthesized either in response to trauma, damage, inflammation, or in response to the cytokines IL-1 or TNF- α .

A subfamily of cytokine is the chemokine, which direct the traffic of leukocytes; during inflammation, some chemokines attract immune cells to the inflamed tissue. Chemokines affect target cells by two mechanisms. First, they alter the cells adhesive abilities so immune cells can adhere to endothelial cells of the blood vessels and enter the inflamed tissue. Second, they attract and direct the movement of these cells toward the centre of the inflammation through a concentration gradient of the chemokines. Two large undergroups of the chemokines are CXC and CC. In CXC, the two N-terminal cysteins are separated with an amino acid ("X"), whereas in CC the cysteins lie adjacent to each other. The different CXC chemokines target either neutrophils or lymphocytes and CC chemokines target a diverse range of cell types, including basophils, dendritic cells, macrophages and eosinophils.

IL-8, also referred to as CXCL8, is a chemokine whose primary role is to recruit neutrophils to inflamed tissue. The neutrophils are the most abundant and lethal phagocytic leukocyte. Phagocytosis is a process of capturing, engulfing and killing microorganisms. They have multiple cytoplasmic granules containing reactive substances enhancing inflammation and making killing microbes efficiently. IL-8 was the first chemokine identified. It is particularly interesting because expression of IL-8 in cells under normal conditions are low, whereas a fast and significant increase in IL-8 levels are seen in response to external stimuli such as pro-inflammatory cytokines (IL-1, TNF- α), microbial products and cellular stress [38]. IL-8 is thought to be a very important cytokine due to its strong neutrophil recruitment ability, an important mechanism in respect to fast innate immune responses.

RANTES, also referred to as CCL5, is a chemokine that recruits multiple types of immune cells, including monocytes, T cells, eosinophils and basophils. It can also activate eosinophils [39]. The latter two make out the three granulocytes together with neutrophils. This indicates a great variety of functions of RANTES, and it might play a role in many different types of infections. Eosinophils are found in respiratory tract, and are thought to be an important mediator of inflammatory respiratory diseases such as asthma.

1.4.2 Acute and chronic inflammation

Inflammation can be divided as either an acute or a chronic process, i.e. an inflammatory process of short or long duration. There are several different features that distinguish these two. The onset of an acute inflammation is fast with leukocyte infiltration of mainly neutrophils, whereas the onset of a chronic inflammation can take up to several days with primarily monocytes, macrophages and lymphocytes as effector cells. One other important difference is that an acute inflammation usually creates a mild and self-limited tissue injury, whereas there is a severe and progressive tissue injury with fibrosis in chronic inflammation.

Acute inflammation is triggered during infections, tissue necrosis due to cell damage, foreign substances/objects or immune reactions. Removal of the cause and tissue repair usually

terminates the inflammation. When cell damage, infection or exposure of a foreign substance/object is persistent on the other hand, chronic inflammation takes place. The inflammatory response is now more dominated by macrophages and lymphocytes (i.e. involvement of the adaptive immune response), following constant tissue destruction by inflammatory cells and mediators with subsequent reparation and replacement by fibrotic tissue. A chronic inflammation starts therefore with an acute inflammation.

1.4.3 Inflammation in the lungs

Inflammation-inducing substances can reach the lungs either through inhalation or through the circulation. The inhaled air contains a lot of foreign substances and microorganisms, making the lungs particularly exposed. The lungs are equipped with antioxidants and antiproteases that can self-limit tissue damage of an inflammatory process. When pulmonary cells die of necrosis, inflammation occurs with a subsequent repair and regeneration of lost cells. An acute inflammation is also especially easy triggered in the lungs due to the thin and fragile type 1 pneumocytes that covers most part of the alveolar surface. Type 2 pneumocytes can proliferate and differentiate to type 1 pneumocytes, making an important contributor of tissue repair and regeneration when the affected cells are type 1 pneumocytes. When an irreversible damage or a persistent exposure of the toxic agent takes place, chronic inflammation occurs with subsequent lung damage.

1.4.3.1 Pulmonary fibrosis

Pulmonary fibrosis is a type of chronic inflammation in the lungs, often developed due to persistent exposure of drugs or occupational pollutants. It is characterized by the replacement and accumulation of fibrotic tissue and extracellular matrix in the lungs. It starts with the release of cytokines and tissue factors from activated neutrophils and macrophages that leads to the proliferation of fibroblasts. This again leads to increased production of extracellular matrix. The stimulation is normally altered when the damaged tissue is replaced. If the stimulation persists, fibrosis occurs. The matrix in fibrosis has an abnormal composition with an increased content of collagen and laminin. In addition to increased production, the

degradation of the matrix is also reduced. The consequence is a smaller and stiffer lung with a reduced capacity for gas exchange.

Silicosis is an example of pulmonary fibrosis caused by inhalation of crystalline silica dust, normally low doses of long-term exposure. Silica is a natural, common material found in most rocks and sand. It is most commonly found in the quartz, but also other types of minerals. Due to its abundance, silica dust is formed during manufacturing, construction work and mining.

Asbestosis is another example of pulmonary fibrosis caused by inhalation of crystalline asbestos fibers. Asbestos consists of six different types of silica minerals. Previously, asbestosis was used in construction work. However, the use of asbestos is now forbidden due to carcinogenic effects.

1.5 Intracellular signalling pathways

The release of pro-inflammatory cytokines leading to inflammation usually requires the activation of specific signalling mechanisms. The processes often require specific transcription factors to be activated. Several intracellular pathways phosphorylate these transcription factors, leading to the synthesis of cytokines. The MAPK- and EGFR pathways are intracellular signalling pathways that are activated by stress.

1.5.1 Mitogen-activated protein kinase signalling pathways

Mitogen-activated protein kinases (MAPKs) are a family of protein serine/threonine (Ser/Thr) kinases that has a central role in both cell homeostasis and inflammation. Protein kinases are enzymes which, when activated, phosphorylate other proteins, usually leading to their activation. Protein kinases are also themselves activated by phosphorylation. MAPKs differ from other protein kinases in that they are proline-directed, i.e. they phosphorylate only

serine- or threonine residues that are followed by proline residues. Due to an external stimulation, downstream cascades of MAPKs are activated. One result is the phosphorylation and activation of transcription factors followed by synthesis of pro-inflammatory cytokines [38, 40-44]. The MAPKs can also phosphorylate other protein kinases than transcription factors [41, 43], both cytoplasmic and in the nucleus. The activation of other protein kinases increases the range of biological function that MAPKs can regulate. One family of protein kinases MAPKs activate is MAPK-activated protein kinases (MAPKAPKs) [43].

There exist multiple MAPK pathways [42, 43], but three major MAPKs signalling cascades, p38, c-JUN NH₂-terminal kinase (JNK) and extracellular signal regulated kinases (ERK), are important both for inflammatory responses and normal cell functions [40-43]. Studies show that especially p38 and JNK to a large extent are activated by environmental stresses and cytokines rather than mitogens, and thus is called stress-activated MAPKs [42]. Examples of stresses and stress-related mediators are UV radiation, oxidative stress, cytokines, osmotic stress and microbial products [40-43].

The MAPK cascades involve a three-tiered “core signalling module” of three protein kinase steps (figure 8) [40-43]. It starts with an extracellular stimulus, binding and activating a particular receptor that activates processes that ends with activation of the first kinase, MAP3K (or MAP3Ks). MAP3Ks are a general name for a broad group of several protein kinase families [41, 42]. They are often activated either through phosphorylation and/or through their interaction with a small GTPase of the Ras/Rho family [43]. Three key events are central for their activation; membrane recruitment, homoligomerization and phosphorylation [41, 42]. MAP3Ks further activate MAP2Ks (or MEKs, MKKs or MAPKK) by phosphorylating serine and serine/threonine, at distinctive positions, simultaneously. These in turn activate MAPKs by also dually phosphorylating distinctive threonine and tyrosine [41-43].

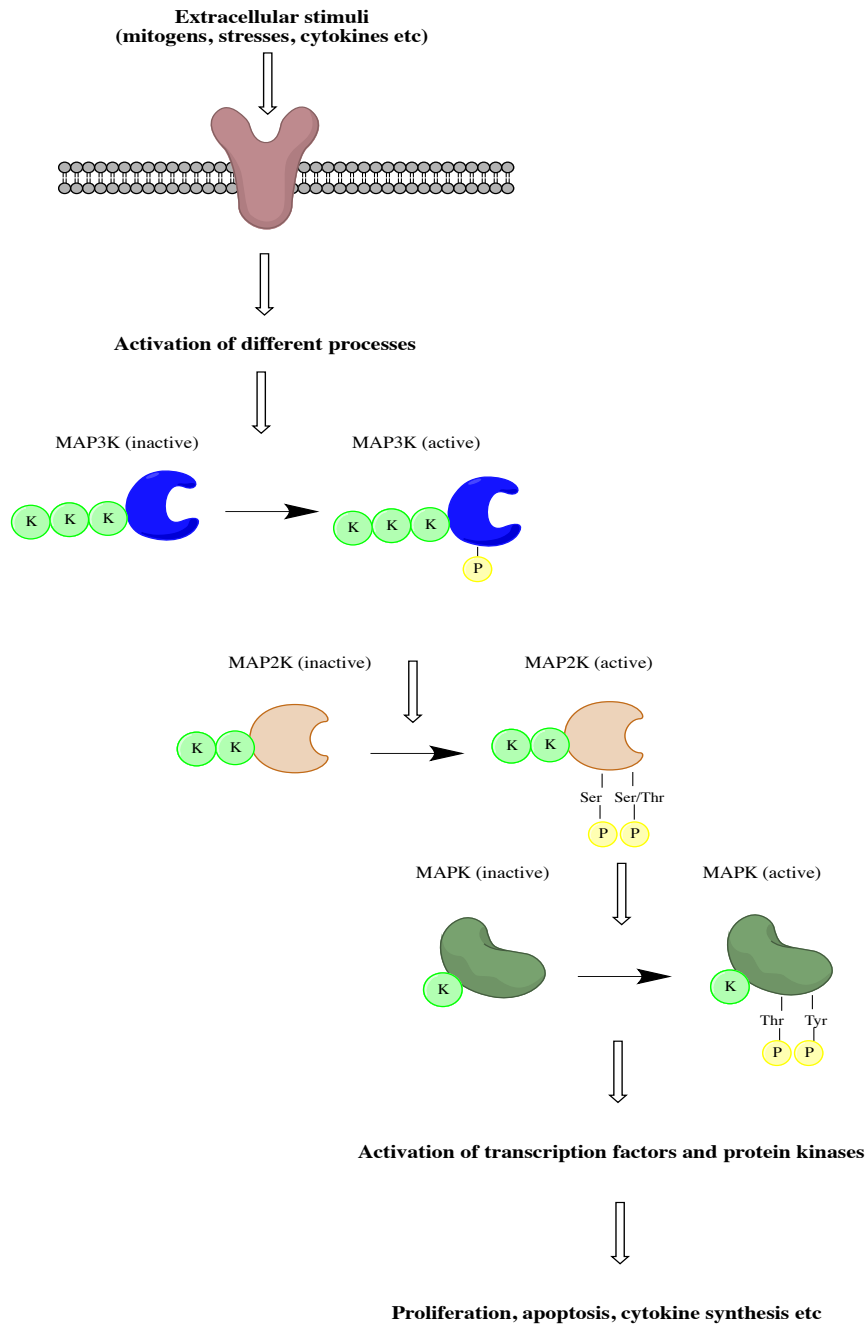


Figure 8: Simplified illustration of the three-tiered MAPKs signalling pathway

Due to specific interactions between MAPKs and their substrates, the different MAPKs have high, distinctive substrate specificity. Activated MAPKs often leads to changed gene expression [40-43]. Each pathway responds to a set of stimuli, enabling the cell to respond specifically depending on the stimulus [41]. However, some of the individual components within the core signalling modules can work across different pathways, and are so regulated

by different stimuli. The different MAPKs have thereby some overlapping activating stimuli, and can also have some overlapping substrates [40-42]. The overlapping substrates mediate thereby both normal cell functions as well as stress-mediated processes [41]. The result is regulation of gene transcription, translation, cell growth, differentiation, apoptosis and other regulatory processes [41-43, 45].

The ERK pathway was the first identified mammalian MAPK. There are two ERKs, namely ERK1 and ERK2 [41-43], both with the same substrate specificity. The ERK pathway is particularly activated by mitogens such as insulin and epidermal growth factor (EGF) [41, 42], as are thereby activated primarily by receptors in the cell membrane, for example receptor tyrosine kinases [43]. It has also been shown that ERK can also be involved in inflammatory processes and be activated by a set of stress and related mediators [42, 43]. In addition to phosphorylate cytoplasmic and nucleus substrates, ERK1/2 can also phosphorylate membrane- and cytoskeleton components [43].

JNK is the second pathway to be identified. There are three different JNKs, each with several isoforms with a total of more than 10 different proteins [41-43]. Even though JNK pathway can be activated by mitogens, it is found that JNK pathway are, to a high degree, activated by environmental stresses, pro-inflammatory cytokines, vasoactive peptides and other toxic substances. JNKs have a different substrate specificity compared to ERK [41, 42]. Like ERK, JNK are involved in controlling cell proliferation. Both MAPKs activate the transcription factor activating protein (AP)-1 which is important regulator of cell proliferation. JNK has shown to induce apoptosis in response to cellular stresses [43].

p38 is another stress-activated MAPKs [40-43]. There are four different isoforms of p38; α , β , γ and δ . They are activated by a set of extracellular stimuli [40-42], particularly inflammatory mediators such as cytokines, chemokines and microbial products [43]. It is shown that most of the stimuli activating JNK also activate p38 [41, 43], and many MAPKs are overlapping between JNK and p38 pathway. p38 also regulates cell proliferation and

survival, and many studies have shown that p38, like JNK, can be implicated in cell apoptosis due to cellular stresses [43].

Studies have shown that, upon activation, a larger proportion of ERK1/2, JNK and p38 are accumulated in the cell nucleus [43]. One of the consequences of MAPK activation is, therefore, the stimulation of the production of many pro-inflammatory cytokines and mediators, for example IL-6 and IL-8, by stimulating transcription factors or stabilizing the produced mRNA [38, 40, 44]. The stabilization is particularly important for the effect of p38. p38 activates MAPK-interacting kinase (MNK)-1 and mitogen-activated protein kinase-activated protein kinases (MK)-2 and -3, members of the MAPKAPKs family [42, 43]. These three proteins regulate cytokine expression by modulating mRNA stability and translation [43]. MK2 for example, can phosphorylate mRNA binding proteins whose functions are to stabilize mRNA, particularly those encoding for pro-inflammatory cytokines [42]. This has been shown for IL-6 and IL-8 [38, 43, 44]. MK2 and MK3 are kinases that are strongly activated by cytokines, stresses and microbial products [42].

1.5.2 Epidermal growth factor receptor (EGFR)

The epidermal growth factor receptor (EGFR) is transmembrane receptor with an intracellular tyrosine kinase activity. This means that, when activated, the kinase phosphorylates only tyrosine residues on its target substrates. Typical ligands of EGFR are growth factors, including transforming growth factor- α (TGF- α). Upon ligand binding, the kinase is activated and phosphorylates both the intracellular C-terminal of the receptor itself and other proteins [46, 47]. EGFR thereby exerts its intracellular effects through the kinase activity [47]. The biological roles include cell proliferation, cell differentiation, migration and survival [45-48]. It is therefore not surprising that EGFR is thought as a central receptor in mediating responses in conditions where tissue repair and growth are in focus. A mutation or abnormal expression of EGFR is implicated in several different conditions such as cancer, bacterial infections and viral infections [49-53].

An example is the stimulation of intracellular signal transductions by phosphorylating effector molecules of respective pathways [46, 47]. Some adaptor- or signalling molecules recognize the phosphorylated tyrosine residues of the EGFR, which function as docking sites for these cellular proteins. Upon substrate binding to the phosphorylated tyrosine residues, they come in close proximity of the EGFR kinase, which can phosphorylate these cellular proteins and activate signal pathways. The phosphorylation of the C-domain is not essential for activation of signal transduction, but greatly increases substrate phosphorylation efficiency as well as aiding a formation of multicomponent signalling complexes [47].

EGFR dimerizes upon ligand binding. It can homodimerize with itself or heterodimerize with another family member, i.e. ErbB2, ErbB3 and ErbB4 (EGFR is also referred to as ErbB1), in a ligand-specific manner. These receptor proteins have different intracellular C-domains, and thereby influence which signalling proteins are recruited and activated. Numerous signalling pathways are thereby regulated by EGFR and its ligands through dimerization [47, 54].

As a protein kinase, it is thought that, like the other, phosphorylation of the EGFR kinase leads to its activation. This is not true for EGFR kinase. It is seen that ligand binding to EGFR leads to an increased kinase activity. It is also seen that receptor dimerization is necessary, but not sufficient, to activate the kinase. A proposed mechanism for the activation of the kinase is that ligand binding triggers a conformation change of the receptor, leading to dimerization and reorientation of the kinase domains, which again increases the affinity for ATP binding and thereby enhancing kinase activity [47].

1.5.2.1 Transforming growth factor (TGF)- α

Seven peptides are identified as EGFR ligands, one of which is TGF- α . All are transmembrane proteins, and it is the extracellular N-terminal domain (“EGF module”) that is the functional part of the ligands and binds the receptor. Whereas it is possible for the ligands to bind the EGFR through juxtacrine (cell-to-cell) signalling [48], more often the EGF module needs to be proteolytically cleaved (ectodomain shedding) at either one or two sites to free the

soluble growth factor ligand [48, 55]. The soluble EGF module can then work autocrine, endocrine or paracrine [48].

One family of enzymes that can cleave the ligands is the membrane proteins called a disintegrin and metalloproteinases (ADAMs). As the name indicates, these are a type of disintegrin metalloproteinases [48, 56, 57], in which their catalytic activity is dependent on a zinc ion in their active sites [57-59]. ADAM17, also referred to as tumour necrosis factor (TNF)- α converting enzyme (TACE), cleaves several membrane-bound EGFR-ligands, one of which is TGF- α [45, 55-59]. TACE is therefore a participant of the EGFR signalling pathway. Free growth factor can then very quickly bind to closely EGFR either by autocrine or paracrine fashion [48, 59]. The released, soluble ligand of TGF- α is referred to as mature TGF- α , whereas the membrane-bound ligand is termed proTGF- α . TACE cleaves proTGF- α at two positions of the extracellular part; the N-proximal site and the membrane proximal site. Both of these needs to be cleaved to release mature TGF- α [55]. Although TACE is thought to be an important contributor of the proteolytic cleavage of proTGF- α , studies have shown that other metalloproteinase(s) have proTGF- α converting enzyme activity [55, 58].

1.5.3 Interplay between signalling pathways

Even though the different pathways can be extinguished from one another, there is a multipart collaboration between the different signalling pathways in which mutual activation is possible. Below is meant as a illustration of the complexity.

EGFR has an ability to activate numerous of proteins, its activation often leads to simultaneous stimulation of multiple signalling pathways, many of which that are connected to each other [47]. One pathway that is regulated by EGFR is the MAPK ERK pathway [46, 47, 54]. A simplified schematic of the activation is the recruitment of the adaptor protein Grb2 to the phosphorylated EGFR, which again interacts with the protein Ras, resulting in Ras-activation. Ras activates the MAP3K Raf-1, ending with the activation of MAPK ERK1/2 EGFR-dependent ERK activation is regulated through negative feedback [47].

EGFR-activated ERK1/2 subsequently activates the transcription factor AP-1, which further stimulates IL-8 transcription [53]. MAPKs JNK and ERK1/2 have also been implicated to be activated partly via Src family kinase (SFK)-dependent EGFR-pathway by fluoride in human epithelial cells [60]. The MAPK p38 pathway has also shown to be activated by EGFR in human gliomas [52] and human middle ear epithelial cells-1 (HMEEC-1) [51] even though it is traditionally not considered activated by EGFR. A study on rhinovirus-infected BEAS-2B cells for example, showed EGFR-independent activation of p38 [53]. Another study indicated that the p38 pathway played an important role in rhinovirus-infected BEAS-2B cells, without assessing whether it was EGFR-dependent or –independent [61].

EGFR can also activate NF- κ B through different signalling pathways [46, 47, 51, 62]. Studies investigating inflammatory mechanisms during bacterial respiratory infections by *Haemophilus influenzae* show that the transcription factor NF- κ B plays a major role in mediating the inflammatory response by activating the transcription of numerous of pro-inflammatory cytokines and mediators such as IL-8 [49-51]. It seems like the degradation of the NF- κ B-inhibitory protein I κ B and activation of p38 pathway stimulates NF- κ B-dependent transcription of pro-inflammatory mediators [49, 50]. What is particularly interesting is that *Haemophilus influenzae* has shown to synergize with tumor necrosis factor (TNF)- α , growth factors or microbes to activate NF- κ B and the production of cytokines, such as IL-8, in three human epithelial cell lines [49, 50]. Without assessing to a particular signalling pathway, RANTES, in addition to IL-8 [63] and IL-6 [39, 63], has been shown to be synthesized in virus-infected bronchial epithelial cells. The release of these cytokines, particularly RANTES, might be the reason why viral infections trigger asthma.

It is not just EGFR that can regulate the MAPKs pathways. As mentioned earlier, there is a dual activation of these pathways. Stress-activated p38 is implicated to stimulate EGFR by activating metalloproteases in human carcinoma cells. Activated EGFR are again showed to stimulate MAPKs ERK1/2 and JNK [45]. Another study showed that ligand-activated EGFR stimulates the ERK1/2 pathway to induce cleavage of proTGF- α , but that p38 also can stimulate ectodomain shedding in the absence of activated EGFR [64].

1.5.4 IL-8 in light of the signalling pathways

IL-8 promoter has three sites for three different transcription factors, C/EBP, NF- κ B and AP-1 [38, 44, 65], and all three need to be bound for maximum IL-8 transcription. It is believed that MAPKs regulate IL-8 mainly by activating these transcription factors and by stabilizing the produced mRNA [65-69]. The activation of transcription factor nuclear factor (NF)- κ B is both required [49, 50] and sufficient to induce IL-8 transcription. Activation of the MAPK ERK1/2 [53], JNK- and p38 pathways [38, 44] has also been proven to increase the synthesis of IL-8. Under normal conditions, there is repression of IL-8 promoter that hinders IL-8 transcription [44]. For maximum IL-8 synthesis, derepression needs to take place, in addition to activation of NF- κ B, JNK and p38 pathway. It is thought that overlapping MAP3Ks can activate all three pathways [38, 44]. Some cytokine stimuli, such as IL-1 and TNF- α , have been reported to induce more than 100-fold levels of IL-8, whereas EGF is not as potent, leading only to a 5- or 10-fold increase [44]. But as mentioned earlier, EGFR can lead to increased IL-8 levels by stimulating NF- κ B and the MAPKs.

Activation of JNK and ERK are believed to activate the transcription factor AP-1. IL-8 promoter has binding sites for both NF- κ B and AP-1. These sites lie in close proximity in the promoter region. It is thought that, upon activation of both transcription factors, a nucleoprotein complex is formed, enabling a multiprotein surface that makes optimal contact with the transcriptional machinery and thereby enable maximal IL-8 transcription [44].

As mentioned earlier, the basal levels of IL-8 under normal conditions are low or undetectable. This is due to two reasons: first is the suppression of transcription under normal conditions prevents the cells to synthesize IL-8. Second is the instability of synthesized mRNA. p38 is implicated in IL-8 synthesis in that it stabilizes produced IL-8 mRNA [44].

Signal transducers and activators of transcription (STATs) are a group of transcription factors, which have been implicated in EGFR signalling [47, 53]. They were first discovered to be

activated by cytokine receptors [47], and regulates proliferation, differentiation, migration, apoptosis and survival [70]. In pulmonary lung diseases, it has been reported that the STATs work cooperatively with the other transcription factors AP-1 and NF- κ B to activate pro-inflammatory mediators, including IL-8 [53].

IL-6 has been shown to be regulated in the same manners as IL-8, indicating that the same signalling cascades involved in regulation of IL-8 gene expression are also relevant for IL-6 [44]. This might not be the whole truth, since it has been shown that IL-6 are influenced differently by the culture medium compared to IL-8 [71]. IL-6 is also able, through its receptors, to activate STATs and all three MAPKs [37]. A recent study also showed a prolonged activation of STAT3 due to association of EGFR with ligand-activated IL-6 receptor. Sustained release of IL-6 can therefore contribute to STAT3's role in cancer and chronic inflammatory diseases [72].

1.6 Silica particles and inflammatory responses

Crystalline and non-crystalline (amorphous) silica has been extensively used in many associations [6-8]. Crystalline silica has in addition been proved to induce serious pulmonary inflammation and cancer. Furthermore, such crystalline silica (quartz) exposure has been shown to induce fibrosis and cancer in occupational settings [73]. Thus, the toxicity and effects of non-crystalline silica is therefore of particular interests and understanding their mechanisms on the cellular level has been a subject of experiments. An *in vivo* study in rats comparing the inflammatory effects of inhaled crystalline, colloidal and amorphous silica dust found that crystalline particles gave persistent inflammation, whereas amorphous and colloidal silica particles only induced transient pulmonary inflammation [74]. Another study on mice indicated that amorphous silica nanoparticles induced dose-dependent transient, severe lung inflammation with subsequent lung injury, fibrosis, leukocyte infiltration, and released several cytokines and chemokines. After 14 weeks the inflammatory process was reduced [75].

We have previously studied how silica nanoparticles induce cytokine responses in epithelial lung cells (BEAS-2B) [76, 77] and alveolar macrophages [78], and that IL-8 is regulated by MAPKs and EGFR in human epithelial lung cells [60, 79]. Gaultieri et al. showed that both plain- and rhodamine-coated SiNP are able to induce up-regulation of several cytokines, including IL-8 and IL-6. The rhodamine-coated particles did not internalize into cytosol, but were rather localized outside the cell. SiNP-induced toxicity was therefore believed to be due to interaction of particles with the membrane. The pro-inflammatory potential was larger for rhodamine-coated than plain silica particles.

It has been demonstrated that activation of JNK, p38, ERK and EGFR may be involved in the induction of IL-8/IL-6 [44, 60, 79]. The signalling mechanisms involved in cytokine release induced by a SiNP of 50 nm size (Si50) were hence examined. In these studies, our group found that Si50 induced transcription of IL-6 and IL-8 in BEAS-2B cells partly through MAPKs p38, NF- κ B and the TGF- α /EGFR-pathway. In addition, p38 seemed to be involved in the activation of EGFR by affecting proTGF- α cleavage [76]. The latter has also been demonstrated in Fischer et al. in which p38 phosphorylates and activates metalloproteases [45].

In terms of particle stability, Gaultieri et al. showed that plain 30- and 50 nm silica particles agglomerate instantly when dispersed in LHC-9 medium, a solution rich in salts and proteins, whereas this was not found in BSA-added particle solutions. We also found that 0.1% BSA and 1% BSA had the same stabilizing effect against agglomeration. In addition, it was found that non-agglomerated (BSA-coated) seemed to mediate less cell responses than agglomerated. The latter might not be due to the direct effect of agglomeration, but rather the concealing effect of BSA on the surface reactivity. This assumption is also supported by Val et al [80]

Kang and Lim showed that 10-20 nm silica nanoparticles induce the same or lesser toxicity compared to a 50 nm silica particle in dendritic cells. The 50 nm particles gave more cytotoxicity, and silica particle of 1-5 μ m, in contrast, gave lesser cell death. They showed

that the silica particles were able to induce production of the cytokine TNF- α , but not IL-6. ERK and p38, but not JNK, in addition to NF- κ B were shown to be involved [81]. Another study found no activation of NF- κ B, JNK or p38, but strong activation of ERK, when BEAS-2B cells were exposed to fumed and porous silica nanoparticles [82].

Oxidative stress is believed to be an important mechanism inducing toxicity. The size-dependent production of ROS by silica nanoparticles is shown in several studies [83-87]. Passagne et al. showed that 20 nm silica induced production of anion superoxide, which can eventually lead to destruction of membrane structure by peroxidation of unsaturated lipids and cell death [88]. Another possible cause of cell death is by apoptosis, in which ROS is known to induce the apoptotic machinery [89]. The same study showed the involvement of MAPKs p38 and ERK1/2 in the induction of IL-8 (JNK was not studied). Wang et al. demonstrated a strong correlation between cytotoxicity and ROS production after exposure to 20 nm silica nanoparticle [90]. Passagne et al. also showed that 100 nm silica particle induces production of more antioxidants compared to 20 nm silica, which might explain why larger particles induces less cytotoxicity compared to smaller particles [88].

The internalization of particles favors ROS production. Several studies have shown to internalize silica nanoparticles through endocytotic pathways [86, 88, 91, 92]. Amorphous silica nanoparticles of sizes 20 and 100 nm were taken up in the cytosol in vesicles, but did not reach the nucleus or other organelles, in kidney cells. The same study also speculates that the high toxicity of 20 nm is due to a larger surface area that promotes more interactions with cell membrane [88]. One study showed the uptake of non-opsonized amorphous silica particle, in the other hand, followed a similar pattern, which also induced endolysosomal leakage and activation of caspase-3; these cellular events are known triggers of the intrinsic apoptotic pathway [93]. It has been speculated that silanol groups (Si-OH) on silica surfaces leads to plasma membrane distortion upon interaction. Some believe this is due to the formation of strong hydrogen bonds between silanol groups and the membrane [92, 94]. This mechanism may also cause the endolysosomal leakage leading to release of lysosomal enzymes that destroys the cell membrane.

2 Aims of the study

We have previously demonstrated that silica nanoparticles (SiNPs) of 50 nm (Si50) and 500 nm (Si500) induced pro-inflammatory responses in human epithelial cells, BEAS-2B. The MAPKs p38 and the TGF- α /EGFR-pathway were suggested to mediate Si50-induced cytokine release, in addition to NF- κ B involvement. The present study aims to acquire a better understanding of the pro-inflammatory and cytotoxic potentials of silica nanoparticles, especially very small silica nanoparticles. Cellular effects of SiNPs of 10 nm (Si10) and 12 nm (Si12) in human bronchial epithelial cells, BEAS-2B, are compared with Si50. We are interested in answering the following questions:

- How is the potential of small-sized amorphous silica nanoparticles (Si10, Si12) to stimulate the release of the cytokines IL-6, IL-8 and RANTES compared to a larger amorphous silica nanoparticle (Si50)?
- Does SiNPs induce cytotoxicity? If so, how is the potential of small-sized amorphous silica nanoparticles (Si10, Si12) to stimulate the release of LDH compared to a larger amorphous silica nanoparticle (Si50)?
- How are the MAPKs p38, JNK and ERK and TGF- α /EGFR-pathway involved in Si10-induced versus the Si50-induced IL-6 and IL-8 release?
- Is RANTES regulated through the same signalling mechanisms as IL-6 and IL-8?
- Which particle properties are likely to be important in inducing the pro-inflammatory and cytotoxic potentials of SiNPs?

3 Material and methods

3.1 Materials

3.1.1 Silica nanoparticles

In this study, three different sizes of commercially produced amorphous silica (silicon dioxide, SiO₂) nanoparticles are used. The 10 nm and 50 nm particles are bought as water suspensions, whereas the 12 nm particle is bought as powder. The particles used are:

Si10: amorphous silica nanoparticle, 10 nm (Kisker Biotech)

Si50: amorphous silica nanoparticle, 50 nm (Kisker Biotech)

Si12: amorphous silica nanoparticle, 12 nm (Sigma-Aldrich)

Table 1 shows the most important properties of Si10 and Si50 from the manufacturer. The manufacturer informs, in addition, that Si10 and Si50 have terminal Si-OH groups. A detailed data sheet does not exist for Si12. The manufacturer informs that the primary particle size is 12 nm (measured by transmission electron microscopy (TEM)), 99.8% trace metal basis.

3.1.2 Other materials used in the study

See Appendix 1.

3.1.3 Solutions used in the study

See Appendix 2.

Table 1. Datasheet for Si10 and Si50.

Properties	Si10	Si50
Size (nm)	10	50
Solid content	25 mg/ml	25 mg/ml
Composition	Amorphous silica particles	Amorphous silica particles
Polydispersity index (PDI)	< 0.2	< 0.2
Shape	Spherical	Spherical
Porosity	Nonporous	Nonporous
Stability	Stable in aqueous buffers and organic solvents Instable in hydrofluoric acid and strong basic media	Stable in aqueous buffers and organic solvents Instable in hydrofluoric acid and strong basic media
Product form	Suspension in water	Suspension in water
Particles per ml	2.4×10^{16}	1.9×10^{14}

3.1.4 Cell line and cell culture medium

This study used a SV-40-transformed bronchial epithelial cell line, BEAS-2B. The cells were bought from European Collection of Cell Cultures (ECACC) in Salisbury in United Kingdom. The cells were grown in LHC-9 medium. During nanoparticle exposure, LHC-9 was replaced by DMEM/F12 medium that does not contain proteins, growth factors, lipids or serum.

3.2 Methods: The principles

3.2.1 Particle characterization with light scattering

The scattering of light differs between different particle sizes, and makes a useful tool in determining particle size, particle size distribution and particle zeta potential.

Light can interact with matter in different ways, i.e. transmission, reflection, absorption, fluorescence and scattering. When the particles are very small, i.e. significantly smaller than the wavelength of the interacting light, the scattering follows Rayleigh scattering theory. This states that the light will induce electronic distortion in the particles, making a dipole, which again will emit in form of scattered light in all directions.

3.2.1.1 Determination of particle size and polydispersity with dynamic light scattering

Nanoparticles in suspension undergo Brownian motion due to the solvent molecules constantly bombarding the particles due to random thermal motion. Due to this constant movement, the light scattered by these moving particles fluctuates over time (i.e. dynamic scattering). Dynamic light scattering (DLS) irradiates a laser with a given wavelength into the particle sample, and measures the intensity of light scattered by the particles as a function of time at specific angle(s). The different intensities over time will then be converted to a hydrodynamic diameter based on the determination of diffusion coefficients through DLS. The light scattering is also dependent on particle size, whereas the scattered light intensity increases with increased particle size. DLS have therefore also the ability to determine different sizes of particles.

When measuring particle size with DLS, an intensity distribution of the results from each measurement is produced based on Stokes-Einstein equation. This formula relates particle motion to particle size;

$$D_h = \frac{k_B T}{3\pi\eta D_t}$$

D_h : hydronamic diameter

k_B : Boltzmann's constant

T: temperature

η : viscosity

D_t : diffusion coefficient

The hydronamic diameter, i.e. particle size, is determined based on these variables. The viscosity, pi (π) and Boltzmann's constant are known and the instrument controls the temperature. The instrument determines the diffusion coefficient. An intensity distribution, which is generated based on light scattering of the sample, is produced as a result. From this, number- and volume distributions are generated. Even though they all illustrate the same, the graphs look different. In number distribution, each particle is weighted equally despite of particle size. A volume distribution, however, the largest particles (most volume) are weighted more.

3.2.1.2 Determination of particle zeta potential with electrophoretic light scattering

Light is irradiated and an electric field applied to the particle samples. Charged particles move towards the oppositely charged electrode with a certain velocity. The principle is based on the Doppler shift effect, which states that objects shift the wavelength of the emitted light when moving. The frequency of the shifts increases with increased movement of the particle, i.e. velocity. With this, the electrophoretic mobility can be determined, and be used to estimate zeta potential and zeta potential distribution.

3.2.2 Western blotting

Western blotting is an analytical technique also based on antigen-antibody interactions. The method is used to detect the presence and incidence of a specific protein in a complex mixture extracted from the cells through cell lysis. Four procedures are of particular importance: cell lysis, gel electrophoresis, immunoblotting and immunodetection.

3.2.2.1 Cell lysis and sample preparation

Cells are frozen to ensure low cell activity, and are thereafter lysed with a complex solution containing buffer, phosphatase and protease inhibitors, chelating agents, detergent and sodium chloride (for isotonic conditions). The samples are further diluted with the solution so that each sample contains the same protein concentration. Glycerol, β -mercaptoethanol and sodium dodecyl sulphate (SDS) is added to all samples in the end. β -mercaptoethanol reduces covalent disulphide linkages in proteins, whereas SDS, in combination with heat, will denature the proteins by disrupting non-covalent bonds. This will make the proteins stretch out in their primary structure. SDS, which is anionic, will bind to the proteins making them anionic too and enabling them to move in the electric field during gel electrophoresis.

3.2.2.2 Gel electrophoresis

The gel electrophoresis' role is to separate the mixture of proteins by molecular size. It consists of polymer subunits and a compound enabling polymerization and cross-linking of polymers. Acrylamide and bisacrylamide are the compounds normally used, and the gel electrophoresis are then referred to as sodium dodecyl sulphate-polyacrylamide gel electrophoresis (SDS-PAGE). SDS is usually added to maintain linearity and the negative charge of the proteins. Substances to initiate the polymerization process are also needed in addition, for instance ammonium persulphate (APS) and TEMED. These processes turn the solution into a solid gel. The different samples are applied in each of their well on top of the gel, an electric field applied, and the proteins wander down the gel towards the positive pole. The proteins are then separated based on their molecular weight with reducing molecular weight downwards. This is done due to an increased retention of movement down the gel the

larger the molecule is. The separation depends on the percentage of acrylamide in the gel, and should be adjusted to the molecular weight of the protein of interest; the smaller the protein is, the higher percentage is needed.

3.2.2.3 Immunoblotting

After separation, the proteins are transferred from the gel to a membrane. The transfer can be done by diffusion, vacuum or electrophoresis. Electrophoresis is preferred due to fast and relatively complete transfer of proteins. Electrophoresis can be done either as wet or half-dry method. The membrane is usually made of either nitrocellulose or polyvinylidene fluoride. They have a high non-specific protein binding capacity, and send out high background fluorescent signal during detection.

3.2.2.4 Immunodetection

After the transfer, the membrane is incubated in blocking solution to avoid nonspecific binding of antibodies. There are many proteins that can be used for blocking, for instance dry milk, tween 20, bovine serum albumin (BSA) and gelatine. After blocking, the membrane is incubated with a specific antibody against the protein of interest for either 1-2 hours in room temperature or cold over night. This is followed by incubation of secondary antibody 1-2 hours in room temperature, which will bind specifically to the primary antibody. Detection is done by labelling the secondary antibody with radioactivity, enzyme, fluorochrome or colloidal gold.

A loading control is done by repeating the process, incubating with another antibody against a protein that is supposed to be in a constant concentration in every sample. When this is done, a stripping procedure needs to be done, breaking the bonds between the proteins and the already bound primary antibody.

3.2.3 Enzyme-linked immunosorbent assay (ELISA)

Enzyme-linked immunosorbent assay, often referred as ELISA, is an analytic technique based on interactions between an antigen and antibody. Both are proteins. An antibody is an animal-derived protein that binds to a specific antigen through the recognition of a particular structure, an epitope, on the antigen. Interactions can therefore only exist between an antibody and a fitting antigen, and not between proteins of the same type.

In this method, the antibody or the antigen are passively adsorbed to a solid phase, and then incubated with a fitting antibody or antigen depending on adsorbed reagent. What is used depends on whether an antibody or antigen is of interest. A colour development takes place through an enzymatic reaction, which are then detected and quantified by a spectrophotometer.

There are four types of ELISA; direct, indirect, competition and sandwich. The two latter are based on the direct and indirect principle. The steps can differ to some extent for the different methods up until addition of the colour development system. Only the indirect sandwich ELISA will be emphasized here.

The sandwich ELISA can only be used to detect antigens. In indirect sandwich ELISA, two different antibodies are used. A coating (also called capture) antibody is adsorbed to a solid-phase. Followed is the addition of our sample with antigen and a detection antibody against the antigen. A protein-enzyme complex is added, whereas the protein binds the detection antibody and the enzyme are responsible for the colour development. Between each step, a washing procedure is done to ensure removal of unbound reagents. Simplified, the process can be described as following:

Step 1: Incubation and passive adsorption of coating antibody to a solid-phase

Step 2: Incubation with blocking dilution to prevent non-specific binding of proteins are available sites on solid-phase.

Step 3: Washing away unbound antibody

Step 4: Addition of sample with antigen. Binding of antigen to coating antibody.

Step 5: Washing away unbound antigen*

Step 6: Addition of detection antibody. Binding of detection antibody to antigen.

Step 7: Washing away unbound detection antibody

Step 8: Addition of colour development system, normally an enzyme-labelled protein and a fitting chromogenic substrate. This protein binds to the detection antibody.

Step 9: Read through a spectrophotometer at 450 nm

*In some kits, step 5 is not necessary, and antigen and detection antibody are added simultaneously.

It is important that the antigen has two different epitopes so that both coating- and detection antibody can bind to the antigen as the method demands. It is also important that these two are species-specific antibodies to ensure optimal recognition and binding of antigen.

Many assays use Streptavidin-HRP (horseradish peroxidase), hydrogen peroxide (H_2O_2) and tetramethylbenzidine (TMB) as the colour development system. Streptavidin is a protein with high affinity to the protein biotin. In assays using this system, the detection antibody is therefore biotinylated, enabling streptavidin-HRP complex to bind to the detection antibody. HRP is an enzyme that can oxidize the chromogenic TMB from colourless to blue by using the oxidizing agent hydrogen peroxide. Quantification is able due to the colour intensity is related proportionally to the extent of HRP activity, which again is related to the antigen levels*. Before reading through a spectrophotometer, a stop solution containing acid (often

sulphuric acid) is added to stop further reactions, turning the colour from blue to yellow (figure 9).

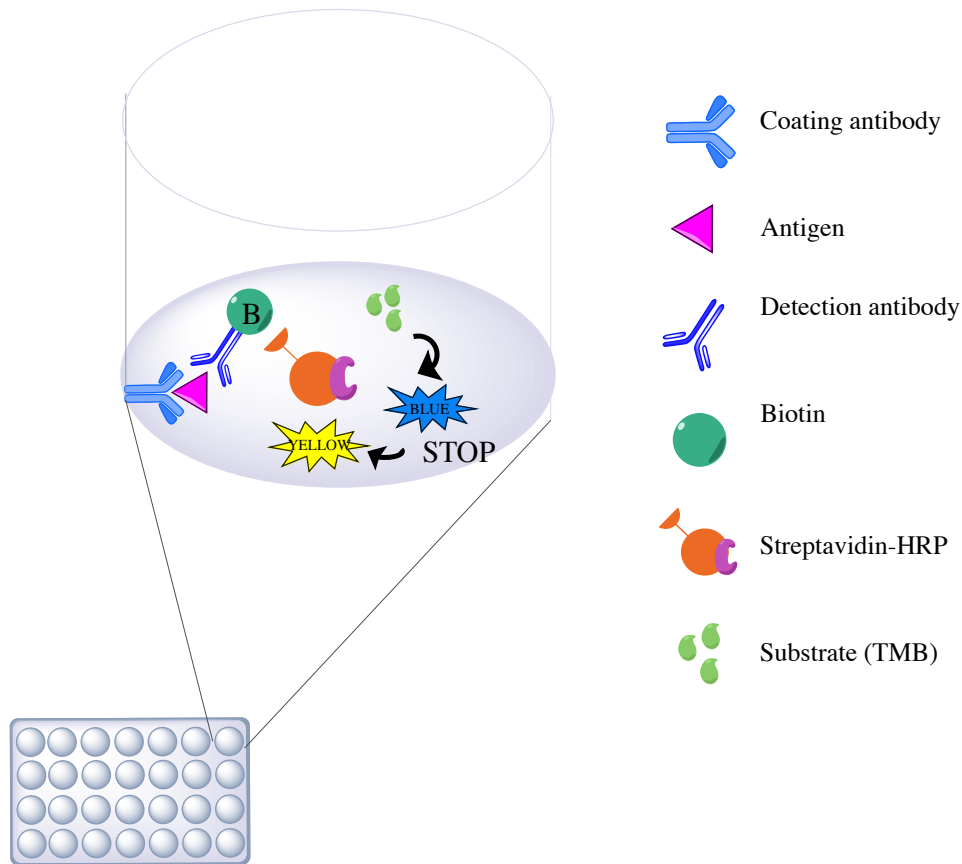


Figure 9: Principle of sandwich ELISA.

3.2.4 Small interfering RNA (siRNA)

Small interfering RNA or silence RNA (siRNA) is double-stranded RNA molecules with 20-25 base pairs. They have the ability to silence the expression of specific genes with complementary nucleotide sequences through post-transcriptional mechanisms. To be able to exert its effect, siRNA needs to get intracellular. The siRNA molecules are brought into the cell through transfection. The transfection reagent in this study, HiPerFect, is a blend of cationic and neutral lipids forming liposomes, which again fuse with the cell membrane and release siRNA on the other side of the cell membrane.

In the cell, the siRNAs integrates into the protein complex RISC, which guides the siRNAs to the target mRNA. The RNase Argonaute 2 (Ago2), which is part of the RISC-complex, degrades the sense strand of the siRNA duplex, leaving only the antisense strand left to bind to a complementary mRNA, i.e. our target. Ago2 can silence gene expression either by inhibiting translation or by destroying the complementary target mRNA through its endonuclease activity, i.e mRNA degradation.

3.2.5 Colorimetric lactate dehydrogenase (LDH) assay

Lactate dehydrogenase (LDH) is a cytosolic enzyme used to analyse cell cytotoxicity. During cell death, the cells will lyse and lose the membrane integrity, releasing cytosolic contents to the environment. Even though LDH is not a direct biomarker for cytotoxicity, the assay determines the leakage of cell contents due to reduced membrane integrity, which is closely related to cell death. The assay determines LDH activity in a coupled enzymatic reaction, reducing the tetrazolium salt INT to formazan, which turns the solution from light yellow to red. Increased formazan production gives increased colour formation.

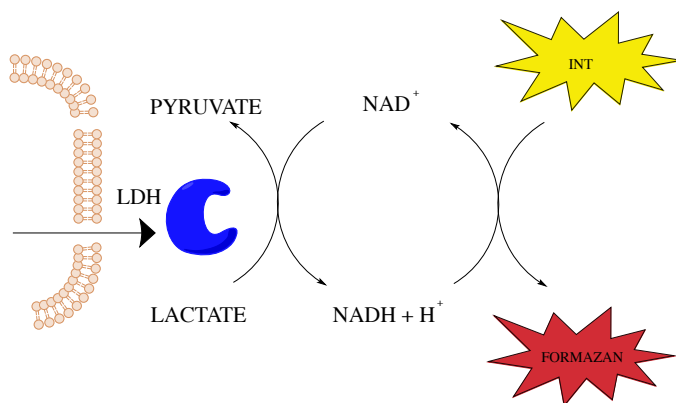


Figure 10: Principle of LDH assay.

3.3 Methods: Procedures

3.3.1 Preparing the particle solutions

The particle solutions of Si10 and Si50 bought from the manufacturer were dispersed in water to a concentration of 2.3 mg/ml. Dry powder of Si12 were weighted and also dispersed in water to a concentration of 2.3 mg/ml. To make it appropriate for *in vitro* research, the particle dispersion was made based on the optimized method of Bihari et al [6]: 1 ml of the stock solution are sonicated with 420 kJ/ml (50% amplitude), first added 34.5 μ l 50 mg/ml bovine serum albumin (BSA) and then 115 μ l 10x PBS. The final particle concentration was 2 mg/ml with 0.15% BSA and 1x PBS.

3.3.2 Cell growth

The BEAS-2B cells were maintained in LHC-9 medium on collagen-treated cell culture bottles. Two days before particle exposure, the cells were plated out in collagen-treated plates. One day prior to particle exposure, LHC-9 was substituted with DMEM-F12 medium. A plate of 6 wells with 1.5 ml medium contained 34.000 cells/cm². A dish with 10 ml medium contained 28.000 cells/cm². The wells/dishes were 80% confluence on the day of particle exposure.

3.3.3 Particle characterization

One 2 mg/ml particle solutions of Si10, Si12 and Si50 were prepared as described in section 3.3.1. Each particle solution was diluted in water and DMEM/F-12 to give three samples with a concentration of 100 μ g/ml. The samples were transferred to cuvettes and the particle sizes and particle size distributions were measured by Malvern Nano ZS at 0 hours using DLS method. The samples in DMEM/F-12 were further incubated for 2 hours at 37 °C and reanalysed. The zeta potentials of 100 μ g/ml Si10, Si12 and Si50 in water were measured by Malvern Nano ZS using ELS method.

3.3.4 Silica nanoparticle exposure to BEAS-2B cells

The BEAS-2B cells were exposed to SiNPs in DMEM/F-12 for 20 hours in the cytokine and cytotoxicity experiments and for 0.5-4 hours in the Western- and TGF- α experiments (table 2). The particle concentrations depended on the type of experiment (table 3).

Table 2. Time point of supernatant harvesting for different experiments

Experiment type	Time point of supernatant harvesting after particle exposure
Western blotting	0.5-, 1-, 2- and 4 hours
Release of cytokines with and without signalling pathways inhibition and siRNA	20 hours
Release of LDH	20 hours
Release of TGF- α	0.5-, 1-, 2- and 4 hours

Table 3. Particle concentrations for different experiments

Experiment type	Si10	Si12	Si50
Western blotting	25 and 50 $\mu\text{g/ml}$	-	100 and 200 $\mu\text{g/ml}$
Release of LDH	0-100 $\mu\text{g/ml}$	0-200 $\mu\text{g/ml}$	0-200 $\mu\text{g/ml}$
Release of cytokines	0-100 $\mu\text{g/ml}$	0-200 $\mu\text{g/ml}$	0-200 $\mu\text{g/ml}$
Release of cytokines with siRNA and inhibition of signalling pathways	25 $\mu\text{g/ml}$	-	200 $\mu\text{g/ml}$

3.3.5 The use of chemical inhibitors

In experiments investigating the involvement of intracellular signalling mechanisms, the BEAS-2B cells were exposed to Si10 and Si50. 1 hour prior to particle exposure, the cells were pre-treated with chemical inhibitors of p38 (SB202190, 20 μ M), ERK1/2 (PD95059, 20 μ M), JNK (SP600125, 20 μ M), TACE (TAPI-1, 20 μ M) and EGFR (AG1478, 10 μ M).

3.3.6 The use of siRNA

siRNA against JNK was additionally done to assess the role of JNK in SiNP-induced cytokine release. BEAS-2B cells were transfected, i.e. treated with mixture of HiPerfect and siJNK, the same day that the cells were plated out on 6-wells plates. Each well contained 250,000 cells in 2.3 ml LHC-9 medium. The transfection mixture for each well contained 100 μ l LHC-9 medium, 6 μ l HiPerfect and 10 nmol siRNA. A non-target siRNA was used as control for off-target effects of siJNK. It is well known that siRNA affects the expression of other non-target genes; controlling with a non-target siRNA will control for the potential misleading results of off-target effects. The transfection mixture is vortexed, rested for 5-10 minutes and then added dropwise to each well. The cells were incubated 24 hours before it is replaced with DMEM/F-12 medium, and exposed to Si10 and Si50 48 hours after transfection. The cell supernatants were harvested after 72 hours. Control cells from 48- and 72 hours were frozen down and later analysed with Western blotting (section 3.2.2).

3.3.7 Analysis of TGF- α release

The cells were pre-treated with anti-EGFR (4 μ g/ml) 30 minutes prior to Si10 and Si50 exposure. Anti-EGFR was needed to block the binding of free TGF- α so that it remained in the medium and assessable for ELISA analysis. The TGF- α levels were analysed with sandwich ELISA (Duoset, R&D systems) according to the manufacturer's procedure.

3.3.8 Sample preparation and procedures for analysis with ELISA and LDH assay

The supernatants from particle-exposed cells were harvested depended on the experiment design and particle exposure duration (see section 3.3.4). After harvesting, the dead cells removed by centrifuging at 1200 rpm for 10 minutes followed by the removal of nanoparticles by centrifuging at 10000 rpm for 10 minutes.

3.3.8.1 Sandwich ELISA

The amounts of IL-6, IL-8, RANTES and TGF- α in the cell supernatants were analysed with sandwich ELISA (Cytoset, Life Technologies/Duoset, R&D systems) according to the manufacturers' procedures. A 96-well microtiter plate was pre-coated with a capture antibody for the target antigen 1 day prior to the analysis. Before adding supernatants, the microtiter plate was washed with PBS and incubated with a blocking solution for 1 hour. 100 μ l supernatant of each sample were applied in a one well in the microtiter plate for 2 hours in a dark room at room temperature while shaking. For IL-6 and IL-8, detection antibody was added at the same time as the supernatants. For RANTES and TGF- α , the detection antibody was added after the 2 hours incubation for another 2 hours after washing the microtiter plate with PBS. After the incubation with supernatants and detection antibody, the plate was washed with PBS, incubated with HRP for 20 minutes, washed with PBS and incubated with TMB, H₂O₂ and citrate buffer. When satisfactory colour development was reached, the reaction was stopped with sulphuric acid and read in a plate reader at 450 nm. The concentrations of the antigen were decided by using a standard curve of the same antigen with known concentrations.

3.3.8.2 The LDH assay

The amounts of LDH in the cell supernatants were measured with a LDH assay (Cytotoxicity detection kit, Roche). 100 μ l supernatant of each sample was applied in a one well in the microtiter plate, added 100 μ l of a reaction mixture and incubated dark for 5-30 minutes until

satisfactory colour development. The plate is read at 450 nm in a plate reader. The amount of cytotoxicity based on LDH release was related to maximum LDH release, where the cells were incubated with Triton X-100 for 1 hour to give 100% cell necrosis.

3.3.9 Western analysis

BEAS-2B cells were exposed to Si10 and Si50 for 0.5, 1, 2 and 4 hours. The supernatants were removed whereas the wells with the cells were washed with cold PBS and then frozen down at each time point. Frozen wells are then put on ice, added lysisbuffer and then scraped for cells. The lysates were then sonicated for 4 times in 30 seconds in a BioRuptor® followed by centrifugation in 10000 rpm for 15 minutes to remove membrane residues. The protein concentration of each sample were then determined with DC-protein assay (BioRad) according to the manufacturer's procedure and then diluted with lysisbuffer, 5x SDS mixture and 10% glycerol to a final concentration between 0.3-1.0 mg/ml, and finally denatured in 95 °C for 5 minutes. 10-25 µg of proteins were applied on a 10% polyacrylamide gel. The electrophoresis was run at 200 V to separate the proteins. The proteins were blotted onto a nitrocellulose membrane, blocked with 3% dry milk and then incubated over night with primary antibody against target protein. HRP-conjugated secondary antibody was added to the Western blot for 2 hours before the blot were treated with a Super Signal West Dura (Pierce) to give chemiluminescence of target protein. The immunodetection was done by reading the chemiluminescent at a documentation platform (Chemi-Doc, Bio-Rad). For the determination of the total protein/ β -actin, the blot was stripped in a mild stripping solution (Chemicon) for 15 min, rinsed in Tris-buffered saline (TBS) solution before incubation with primary antibody against the total protein over night. The procedure was then repeated as described above.

3.4 Statistical considerations

There is necessary to ensure that reported effects are, in fact, true results. Statistical analysis is used to document that differences between compared groups are not due to coincidental circumstances. The difference between groups is significant if there is a 95% probability that the groups are not like. Statistical analysis calculates a p-value to indicate the degree of significance, which can be defined as following:

$p = 0.05$: 95% probability that the difference between the compared groups are significant.

$p = 0.01$: 99% probability that the difference between the compared groups are significant.

$p = 0.001$: 99.9% probability that the difference between the compared groups are significant

In the present study, only the 95% probability of significance is reported to simplify the results. Some of these results can, however, have higher probability of significance.

Parametric and non-parametric statistical tests can be used depending on the data. Parametric tests are used when the dataset follow a normal distribution. In this study, we used parametric one-way ANOVA tests and assume normally distributed data. It is however important to notice that there is limited repetition of experiments that normal distributions cannot be ensured. Few repetitions of measurements affect the statistical analysis in which spread of data due to, for instance, different cell density and cell line passage numbers, influences the significance between the groups. Even though the results indicate a difference, large standard deviations make it hard to determine if the difference is significant. For datasets with large variations, statistical analyses were done on log transformed data.

In the present study, the software GraphPad Prism version 6 was used for statistical analysis.

3.5 Methodological considerations

3.5.1 Theoretic particle number in 2 mg/ml Si10 and Si50 particle solution

Based on the data sheet given by the manufacturer, some roughly calculations can be done to assess number of particles per ml (table 4):

Table 4. Calculated number of particles in three different particle solutions of Si10 and Si50.

	Si10 (particles/ml)	Si50 (particles/ml)
From manufacturer:	2.4×10^{16}	1.9×10^{14}
25 mg/ml		
Stock solution:	2.2×10^{15}	1.7×10^{13}
2.3 mg/ml		
Particle solution:	1.9×10^{15}	1.5×10^{13}
2 mg/ml		

3.5.2 Theoretical surface area of 25 µg/ml Si10 and 200 µg/ml Si50 exposed to the cells

The surface area of Si10 and Si50 can be calculated from the formula of the surface area of a sphere: $A = 4\pi r^2$.

The calculated surface areas were 314.2 nm^2 for Si10 and 7854 nm^2 for Si50.

The cells are exposed with 25 µg/ml of Si10 2 mg/ml particle solution. The number of particles at this concentration is estimated to be 2.3×10^{13} based on the calculations in section 3.5.1. This gives a surface area of 7.3×10^{15} . The cells are exposed with 200 µg/ml of Si50 2

mg/ml particle solution. The number of particles at this concentration is 1.5×10^{12} . This gives a surface area of 1.2×10^{16} .

3.5.3 Particle characterization of Si10 particle solution with DLS

Characterization of Si10 particle solution showed inconsistency between the three parallels measured (not shown). The software generates a quality report of each measurement, which supports this assumption. For each of the three measurements of Si10, this “expert advice” believes that there is a polydisperse solution with the existence of large, sedimenting particles. This indicates that the Si10 particle solution is not stable, making it challenging to rely on the results. The errors warn about relying on the produced z-average, polydispersity (PdI) value and/or distribution analysis, and that the samples may not be suitable for DLS measurements. The interpretations of Si10 results are therefore done carefully, and we have chosen to rely on the overall results rather than the individual values, in which there is a polydisperse solution with the existence of agglomerates. Other characterization techniques should be used in addition to get a better understanding of the properties of Si10.

3.5.4 The preparation of particle solution – is it optimal?

As described earlier, nanoparticle dispersion with physiologic properties is necessary when studying their effect on cells (section 1.1.3). This, however, often leads to agglomeration of individual particles. Since it is believed that the size of nanoparticles is an important factor affecting biological responses, agglomeration to larger particles will alter their effects. Further processing of the particle solution may modify the particles bought from the manufacturer and deviate from the technical details given. This, again, implies the importance of proper particle characterization when studying nanoparticles biological- and toxic effects.

Due to the agglomeration of nanoparticles in physiological solutions, an optimized dispersion method is needed to ensure best possible stability. Bihari et al concluded the following based on their study [6]:

- It is necessary to sonicate with enough energy to deagglomerate particles ($>4.2 \times 10^5$ kJ/m³).
- Addition of albumin or serum as stabilizer at a sufficient high concentration that the nanoparticles are completely covered (1.5 mg/ml albumin/serum for 2 mg/ml dispersions).
- Optimal preparation sequence:
 1. Sonication of nanoparticles in distilled water
 2. Add stabilizer
 3. Add PBS

In our study, Bihari et al. method was used for particle solution preparation. The BSA functioned as the steric stabilizer, adhering to particle surface and prevents particle agglomeration. PBS was added so the suspension mimicked physiological conditions.

The sequence of the steps is of particular important. Sonification has to be done first to deagglomerate particle aggregates. Adding BSA after sonification, but prior to PBS, stabilizes the individual particles after the deagglomeration of the sonification. It is important that PBS is added after BSA to avoid reagglomeration due to the electrolytes and pH [6].

Bihari et al. believed that this dispersion method led to a stabilized dispersion without agglomeration. The pH and electrolyte concentrations of physiological solutions do not provide a large enough zeta potential to prevent agglomeration, i.e. ± 30 mV. This might seem contradictory to our current results and will be discussed below (section 5.1). It is therefore necessary to use steric stabilizer, not electrostatic stabilizers, to optimize the stability in a

nanoparticle dispersion. It should also be noted that the authors of the article commented that the method was not that effective for silica oxide nanoparticles.

Bihari et al. also described that a 2 mg/ml solution of titanium dioxide (TiO₂) nanoparticles gave increased average diameter and PDI value in DLS measurements, but this was avoided when amount of albumin was increased by 10 times. Too low concentration of albumin might be a theoretical reason why the agglomeration of Si10 and Si12 particles, in which the particle surface is not fully coated and enable close contact between the particles.

Based on our calculations of particle surface area from section 3.5.1 and 3.5.2, a 2 mg/ml Si10 has a theoretical total surface area of 5.9×10^{17} , whereas 2 mg/ml of Si50 has 1.2×10^{17} . This means that there is more surface area in the Si10 particle solution compared to Si50 solution, and that the BSA amount used for preparing Si50 solution (which seems stable when measured with DLS) may be inadequate for Si10.

The use of PBS in particle solution can also be a possible problem. The salts in PBS have showed to stimulate agglomeration of nanoparticles [95]. For Si50, this was not true in this and previous study [77]. However, there is a possibility that Si10 and Si12 are more sensitive, and thereby agglomerate to a larger extent.

In addition, Mahmoudi et al. showed that *in vivo* temperature fluctuations, i.e. 37-41 °C, affected the protein corona formation and composition significantly [24]. During our study, the particle solutions are sonicated (i.e. heated up), kept at a cold temperature (4-8 °C) and exposed to cells and kept at 37°C. There is therefore a great chance that the protein corona changes during this course of changes. More importantly, there is a possibility that the SiNPs in particle characterization do not have the same properties as the particles exposed to the cells.

3.5.5 The stability of a new and old Si10 particle solution

To assess whether or not our particle solution is stable, a one week old and one new particle solution of Si10 was exposed to cells and compared. Figure 11 shows that the particle solution is relative stable for one week. The results indicate that the particle solution is stable for at least 1 week.

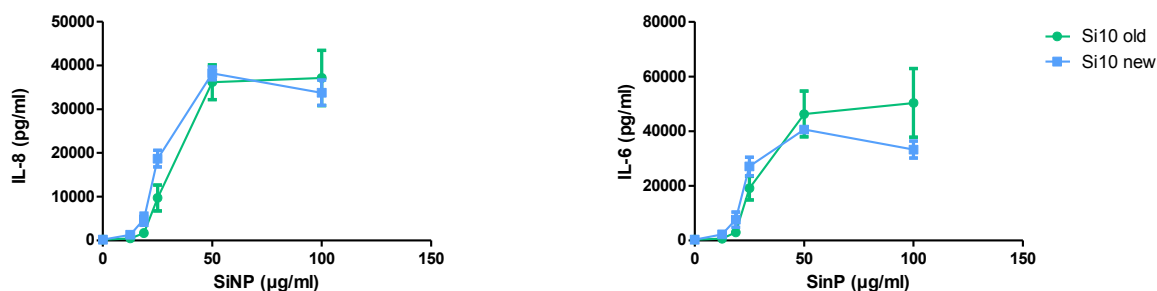


Figure 11. Comparison between one week old and newly made particle solution of Si10.

3.5.6 Consideration of cell medium

As mention in section 3.3.2, the cells were grown in LHC-9 medium, but the medium was changed to DMEM/F-12 one day prior to particle exposure. The medium during particle exposure was also DMEM/F-12. DMEM has previously been used to disperse and stabilize a wide variety of nanoparticles, including metal nanoparticles, metal oxide nanoparticles and carbon nanotubes [96]. The change of medium was made due to different effects of LHC-9- and DMEM/F-12 medium that was shown in a previous study. The addition of serum in the medium also gave remarkably reduced cytokine release [71]. Biological medium and temperature have been shown to influence the formation and composition of the protein corona, which thereby affects the particle reactivity, agglomeration and the followed effects [23, 24]. Cell medium can therefore influence the nanoparticle-cell interactions, and alter the effects. This again illustrates the influence for how biological fluid can affect the resulting effects of nanoparticles.

4 Results

4.1 Characterization of size and charge of silica nanoparticles

From one 2 mg/ml particle solution, three different particle solutions were diluted with water and DMEM/F-12 to 100 $\mu\text{g/ml}$ and analysed individually for particle size and charge. Figure 12 shows the results for all three particles (Si10, Si12 and Si50) from one measurement in DMEM/F-12 and the particle charge measured in water. The particle charges, i.e. the zeta potential, were negative with only small differences between the different particle sizes.

The DLS measurements showed three different size populations of Si10 with diameters of 16 nm, 120 nm and 913 nm when measured with “size by intensity” in medium at 0 hour. This shows that the particles agglomerate in media and give agglomerates consisting of different amounts of particles. It also seems that the size of the agglomerates changed over time, since the measurement after 2 hours showed an even more agglomerated solution. When the size distributions are presented by number, only one size distribution of approximately 10 nm shows at both 0 and 2 hours. This indicates that most of the particles by number seemed to be at this size. Larger particles give larger light scattering than smaller particles, which might explain why the size distributions by number only indicate small particle sizes. The large intensity size distribution at ~ 100 nm should therefore only be interpreted as if there are large agglomerates present. It should be noted that the shown graphs might not be representative, as the results differed between three parallels measured (data not shown). DLS measurements of Si12 particle solution show only the presence of one size distribution, both by intensity and number, with the average size of approximately 250 nm at 0 hour, which is over 20 times the declared TEM-size from the manufacturer. This is probably due to agglomeration of the nanoparticle both in media and water, contributing to non-nanosize distribution. The Si12 showed a reproducible particle solution, as there was consistency between the results of the three sample measured. It also seemed as incubation in DMEM/F-12 for 2 hours at 37 °C further increased the mean particle size. Si50 seemed to be the most reproducible particle

solution, as the parallels showed similar results. In addition, no agglomerates were detected. The Si50 showed little difference between the particle solutions in DMEM/F-12 between 0 hour and 2 hours, although it seemed to be a slight reduction of particle size and polydispersity after 2 hours. The extent of polydispersity is represented by the polydispersity index (PDI). Since it for Si50 is not 0, there existed particles of different sizes in the particle solution, as also indicated by the standard deviations. The values from the measurements are shown in Table 5. Measurements data with respective size distributions graphs in water for all three particles are shown in Appendix 3.

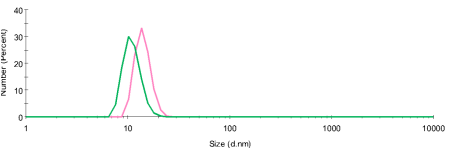
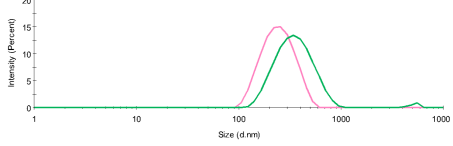
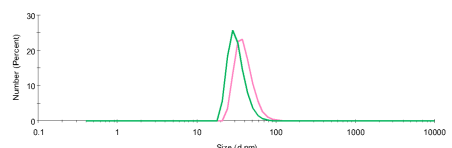
SiNP	Size distribution by intensity	Size distribution by number	Zeta potential (mV)
Si10			-41,6
Si12			-39,3
Si50			-35,1

Figure 12. The size distributions and particle charge of 100 µg/ml of Si10, Si12 and Si50. The hydrodynamic sizes of the different nanoparticles in DMEM/F-12 culture medium are measured by dynamic light scattering (DLS). Both intensity distribution and number distribution are presented. The measurement of one out of three samples is shown. Pink curves represent particles in DMEM/F-12 at 0 hour, whereas green curve represents the same particle solution in DMEM/F-12 after 2 hours incubation at 37 °C. In the right panel, the particle charge (zeta potential) of each particle size in water is presented.

Table 5. Measurement values of Si10, Si12 and Si50 in DMEM/F-12 medium at 0 and 2 hours.

The table shows the measured values of the hydrodynamic sizes of the different nanoparticles. The z-average diameter in addition to the mean diameter with standard deviation of the different size distributions are presented for each particle size. The percentage values indicate the percentage intensity of each size distribution. The polydispersity indexes (Pdl) are also presented.

Sample	Time point	Z-Average (d.nm)	Pdl	Peak 1 (diameter ± st.d., % peak intensity)	Peak 2 (diameter ± st.d., % peak intensity)	Peak 3 (diameter ± st.d., % peak intensity)
Si10 100 µg/ml in DMEM/F-12	0 hour	232.5 nm	0.424	119.6 ± 21 nm 59.8%	16.0 ± 2.5 nm 32.9%	912.7 ± 122.4 nm 7.3%
	2 hours	85.18 nm	0.306	124.8 ± 55 nm 93.3%	13,51 ± 3 nm 6.7%	-
Si12 100 µg/ml in DMEM/F-12	0 hours	221.5 nm	0.163	252.1 ± 61 nm 100%	-	-
	2 hours	319.9 nm	0.215	411.6 ± 200 nm 100%	-	-
Si50 100 µg/ml in DMEM/F-12	0 hour	62.81 nm	0.138	72.86 ± 27 nm 100%	-	-
	2 hours	47.48 nm	0,098	52.98 ± 17 nm 100%	-	-

4.2 The release of cytokines

The pro-inflammatory potential of the three different sizes of silica nanoparticles (10 nm; Si10, 12 nm; Si12, 50 nm; Si50) were first assessed by studying the release of pro-inflammatory cytokines from the nanoparticle-exposed BEAS-2B cells.

As mentioned earlier, cytokines are always involved in harmful events and conditions, regulating inflammatory- and immune responses (section 1.4.1). It is therefore reasonable to first evaluate whether or not the nanoparticles induce cytokine release when characterizing their pro-inflammatory potentials. IL-6 and IL-8 were the cytokines used as pro-inflammatory markers and were chosen to get a better understanding of the nanoparticles' effects on the epithelial cells.

BEAS-2B cells were exposed to increasing concentration of silica nanoparticles of 10 nm (0-50 µg/ml), 12 nm (0-200 µg/ml) and 50 nm (0-200 µg/ml). After 20 hours, the supernatants were analysed for the release of IL-6 and IL-8 with sandwich ELISA (*figure 13*). There was a clear difference in the extent of cytokine release between the different sizes of silica nanoparticles. Si10 induced highest levels of both IL-6 and IL-8 with a significant increase already at 12.5 µg/ml. 25 µg/ml Si10 gave significantly higher increase of IL-6 levels compared to the same dose of Si12 and Si50. For IL-8, the three highest doses for Si10 gave significantly higher increase of the levels compared to the same doses of Si12 and Si50. This study shows a greater increase of these cytokines upon reduced particle size (Si10>>Si12>Si50) on mass basis. This indicates a difference between their reactivity. Interestingly, there was a large difference between the pro-inflammatory potential, i.e. cytokine release, of Si10 and Si12 with regard to the size difference. This was particularly evident for IL-8. There was also a marked difference between the ability of the three SiNPs to induce the release of RANTES. Furthermore, all three particles showed lower responses of RANTES than IL-6 and IL-8. For Si10 and Si50, the pattern of release was similar to IL-6 and IL-8. Si12, however, was not more potent than Si50 in inducing RANTES release. The levels of RANTES were reduced at the highest concentrations used for all three particles,

which is different than for IL-6 and IL-8. This was particularly evident for Si10 in which the level of RANTES was reduced at concentrations above 25 $\mu\text{g/ml}$.

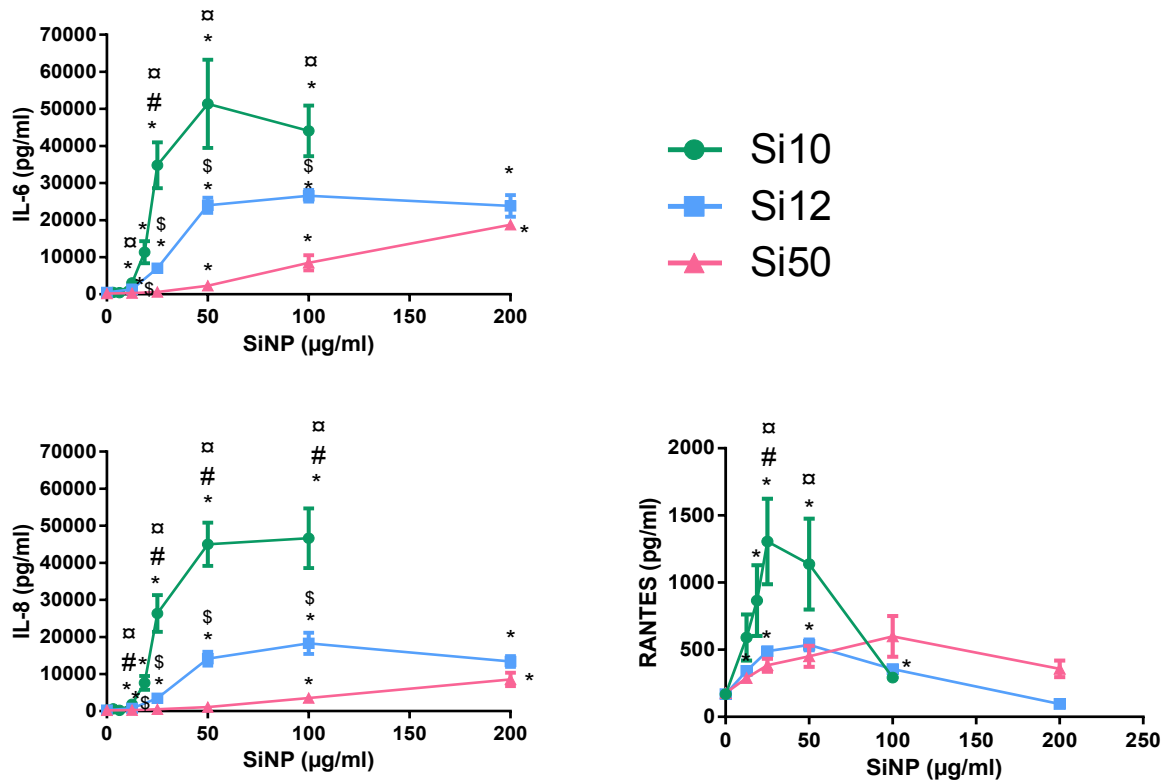


Figure 13. Release of IL-6, IL-8 and RANTES after exposure to Si10, Si12 and Si50 in BEAS-2B cells.

The cells were exposed to the SiNPs for 20 hours, and IL-6, IL-8 and RANTES in DMEM/F-12 medium were measured by ELISA as described. The data represent the mean \pm SEM for at least four experiments. * is significant different compared to control, $p < 0.05$ for Dunnett's one-way ANOVA. # is significant different for Si10 vs Si12, $p < 0.05$ for Tukey's one-way ANOVA. □ is significant different for Si10 vs Si50, $p < 0.05$ for Tukey's one-way ANOVA. \$ is significant different for Si12 vs Si50, $p < 0.05$ for Tukey's one-way ANOVA.

4.3 Cytotoxicity

The cytosolic enzyme lactate dehydrogenase (LDH) is normally analysed in *in vitro* studies as an indicator of cell cytotoxicity. In this particular study, where we are mainly interested in the pro-inflammatory ability of nanoparticles, the characterizing of cell viability also give a better understanding of the nanoparticles' cytotoxic potential.

The release of LDH increased with increasing concentrations of SiNP (*figure 14*).

Furthermore, the particle size influences the toxic potential of the nanoparticles, since the smallest nanoparticle resulted in highest cytotoxicity. There was, however, only a slight, and mostly not significant, difference between the LDH levels of Si10 and Si12. This difference was much less pronounced in the release of cytokines.

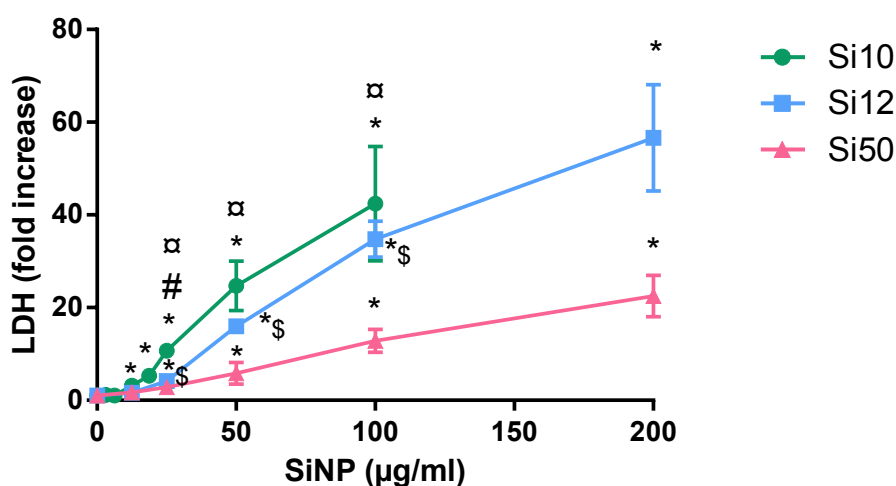


Figure 14. The release of LDH after exposure to Si10, Si12 and Si50 in BEAS-2B cells.

The cells were exposed to SiNPs for 20 hours and LDH release in DMEM/F-12 medium was measured with a LDH detection kit. The data represent the mean \pm SEM for at least four experiments. The results are shown as fold increase of control. Max LDH was 274-fold increased from control (mean of 3 experiments). * is significant different compared to control, $p < 0.05$ for Dunnett's one-way ANOVA. # is significant different for Si10 vs Si12, $p < 0.05$ for Tukey's one-way ANOVA. \square is significant different for Si10 vs Si50, $p < 0.05$ for Tukey's one-way ANOVA. \$ is significant different for Si12 vs Si50, $p < 0.05$ for Tukey's one-way ANOVA.

4.4 Involvement of intracellular signalling pathways in the cytokine release

The next step in our study was to identify which signalling proteins pathways are involved in the release of cytokines, i.e. in mediating of the nanoparticles' pro-inflammatory potential. The concentration 25 µg/ml of Si10 and 200 µg/ml of Si50 were chosen for further investigations based on preliminary results. At these concentrations, it was marked high pro-inflammatory responses, but more moderate changes in cell viability. For the activation of MAPKs, 50 µg/ml Si10 and 100 µg/ml Si50 were additionally used. The signalling proteins studied were the three MAPKs, EGFR and TGF- α because they belong to important stress-activated signal transduction pathways (section 1.5).

4.4.1 Involvement of MAPKs pathways in cytokine release

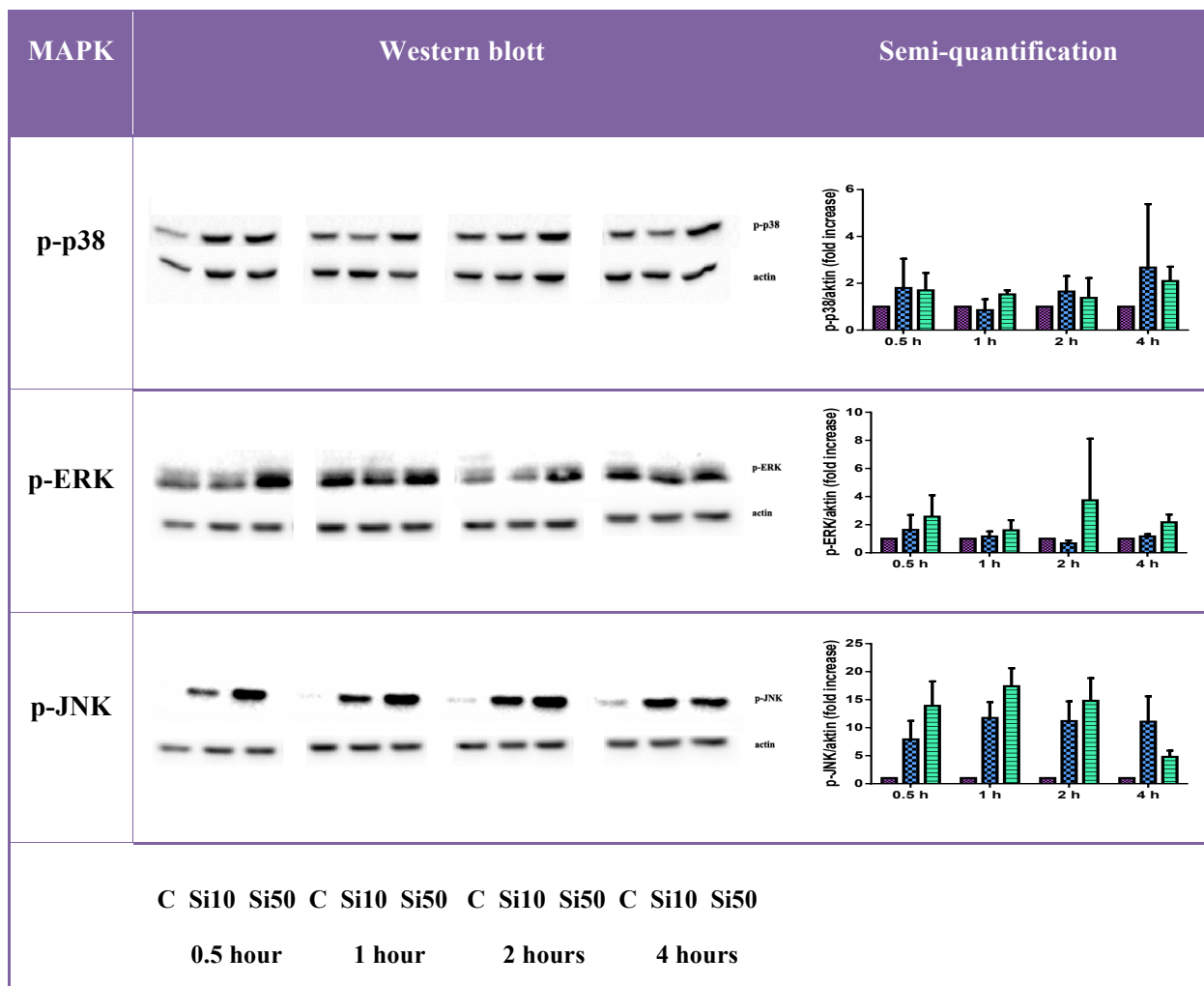
The MAPKs are important signal proteins that, when activated, leads to synthesis of pro-inflammatory mediators such as cytokines. It is therefore of interest whether if the silica nanoparticles activate these stress-activated pathways.

4.4.1.1 Activation of MAPKs after exposure to Si10 and Si50

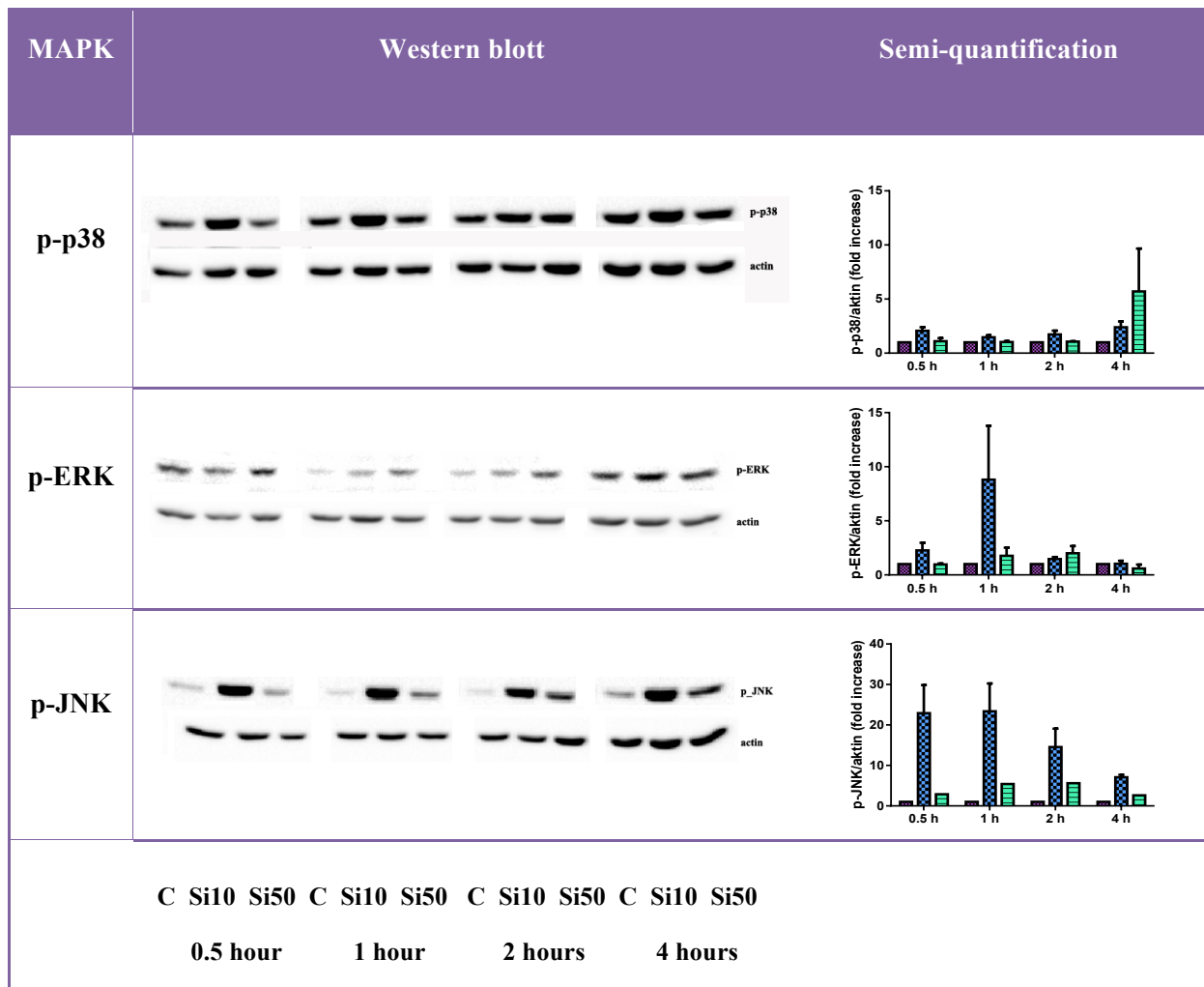
The activation of proteins in cells due to SiNP exposure can be done through Western blotting, in which phosphorylation and phosphorylation pattern of proteins are studied. BEAS-2B cells were exposed to Si10 (25 and 50 µg/ml) and Si50 (100 and 200 µg/ml) for 0.5-, 1-, 2- and 4 hours. The resulting Western blots with semi-quantification (*figure 15 A and B*) show an increase in phosphorylation for all three MAPKs for both Si10 and Si50. The results were very pronounced for JNK, but less distinct for p38 and, especially, for ERK.

For p38, the semi-quantification indicated an early phosphorylation after 0.5-1 hour and a prolonged phosphorylation up to 4 hours. There was not a notable difference between 25 µg/ml Si10 and 200 µg/ml Si50 (figure 15 A). However, 50 µg/ml Si10 seemed to activate

p38 to a larger extent than 100 $\mu\text{g/ml}$ Si50 at 0.5-1 hour (figure 15 B). Si50 seemed to activate p-ERK to a larger extent than Si10, and a phosphorylation was already seen after 0.5 hour (figure 15 A). JNK were strongly phosphorylated from 0.5 to 4 hours for both SiNPs. Which SiNP was the most marked JNK activator was dependent on the concentration. Exposure to 200 $\mu\text{g/ml}$ Si50 gave stronger phosphorylation compared to 25 $\mu\text{g/ml}$ Si10 at 0.5-2 hours (figure 15 A), whereas 50 $\mu\text{g/ml}$ Si10 resulted in much stronger phosphorylation than 100 $\mu\text{g/ml}$ Si50 (figure 15 B). For a better illustration of the dose-dependent activation of MAPKs, see figure 16.



A.



B.

Figure 15. Western blotting of phosphorylated MAPK after exposure to Si10 and Si50.

The cells were exposed to different concentrations of Si10 and Si50 for 0.5-4 hours. B-actin was used as control. Representative blots for each analysis are shown and semi-

quantification with mean \pm SEM from 3 independent experiments. C: control p-p38:

phosphorylated p38 p-ERK: phosphorylated ERK p-JNK: phosphorylated JNK

A. The cells were exposed to 25 μ g/ml Si10 and 200 μ g/ml Si50

B. The cells were exposed to 50 μ g/ml Si10 and 100 μ g/ml Si50

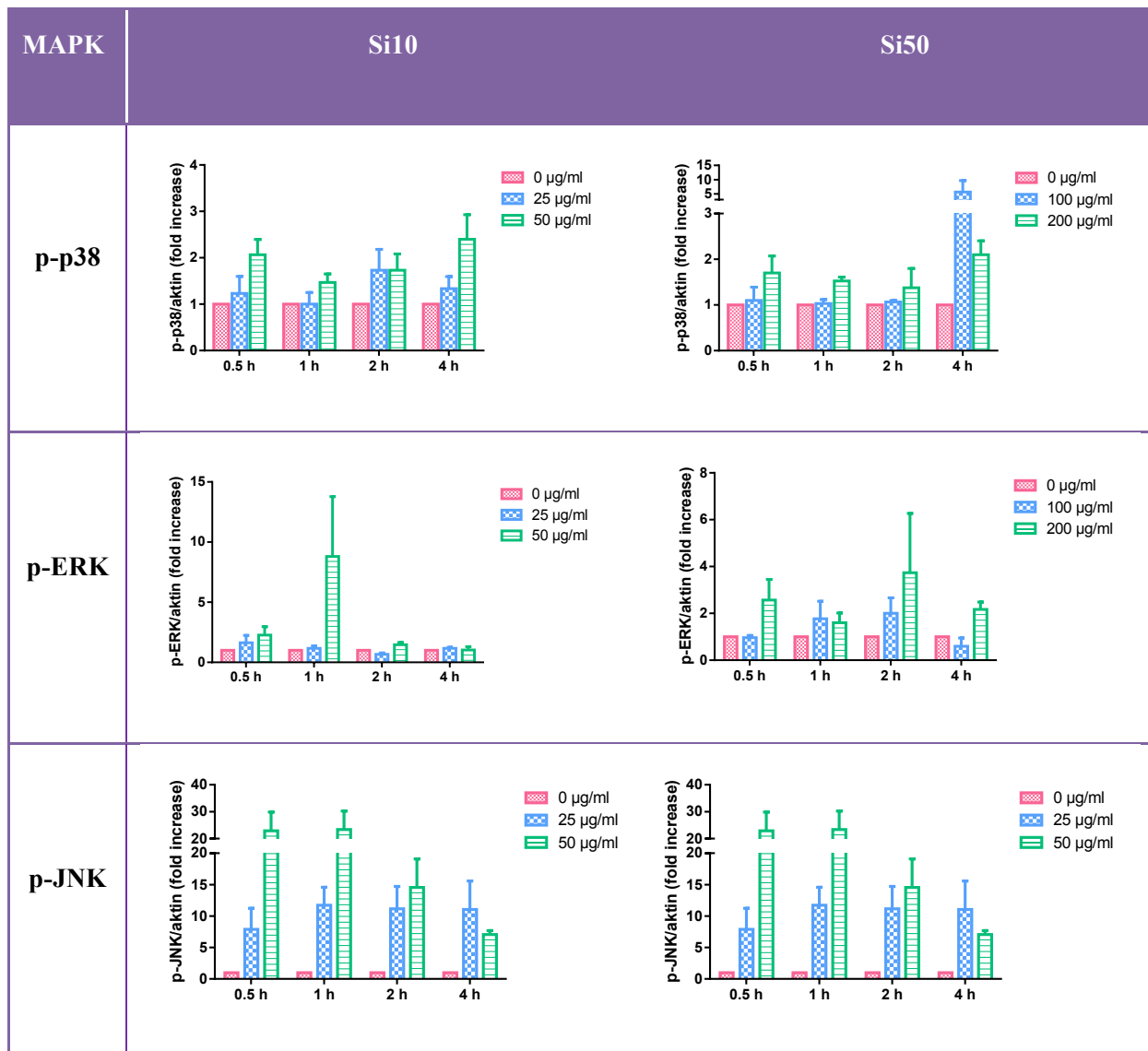


Figure 16. Concentration-dependent phosphorylation of p38, ERK and JNK.

Semi-quantification of the Western blots showing two different concentrations for each particle size; 25 and 50 $\mu\text{g/ml}$ for Si10 and 100 and 200 $\mu\text{g/ml}$ for Si50. B-actin was used as control. Results represent mean \pm SEM from 3 replicates. p-p38: phosphorylated p38
 p-ERK: phosphorylated ERK p-JNK: phosphorylated JNK

4.4.1.2 The involvement of MAPKs in cytokine release

The BEAS-2B cells were pre-treated with chemical inhibitors of the signalling proteins p38 (SB202190, 20 μ M), ERK1/2 (PD95059, 20 μ M) and JNK (SP600125, 20 μ M) 1 hour prior to Si10 (25 μ g/ml) and Si50 (200 μ g/ml) exposure for 20 hours. As shown in figure 17 A, the inhibitors of MAPKs p38 and JNK reduced the release of IL-6 and IL-8 for both Si10 and Si50. The extent of the reduction was approximately the same for both particles for both cytokines. The reduction was particularly evident for p38 inhibition with a reduction of cytokine release of approximately 70% of the maximal response. For JNK inhibition, the levels reduced by approximately 30%. In contrast, the inhibitor of ERK1/2 did not reduce the cytokine release for either Si10 or Si50. The release of RANTES, on the other hand, may indicate the involvement of all three MAPKs for both particles, but the reductions are not significant (figure 17 B).

Besides inhibition of JNK with a chemical reagent, we also used siRNA against JNK (siJNK) to assess the involvement of JNK. The cells were transfected, as described in section 3.3.6, two days prior to particle exposure. The samples were analysed for IL-6 and IL-8 release with sandwich ELISA. Western blotting was used to control the transfection efficiency after 48 and 72 hours. As shown in figure 18 A, the Western analysis showed good transfection efficiency after 72 hours, in which there was a good knock down of the JNK protein. The levels of IL-6 and IL-8 release were lower in the transfected culture (siNT) compared to the control culture, and there was not additive inhibition using siRNA against JNK (figure 18 B). This experiment could indicate that JNK has an uncertain role in mediating particle-activated cytokine synthesis. However, the result shown is based on only one experiment and should not be paid too much attention.

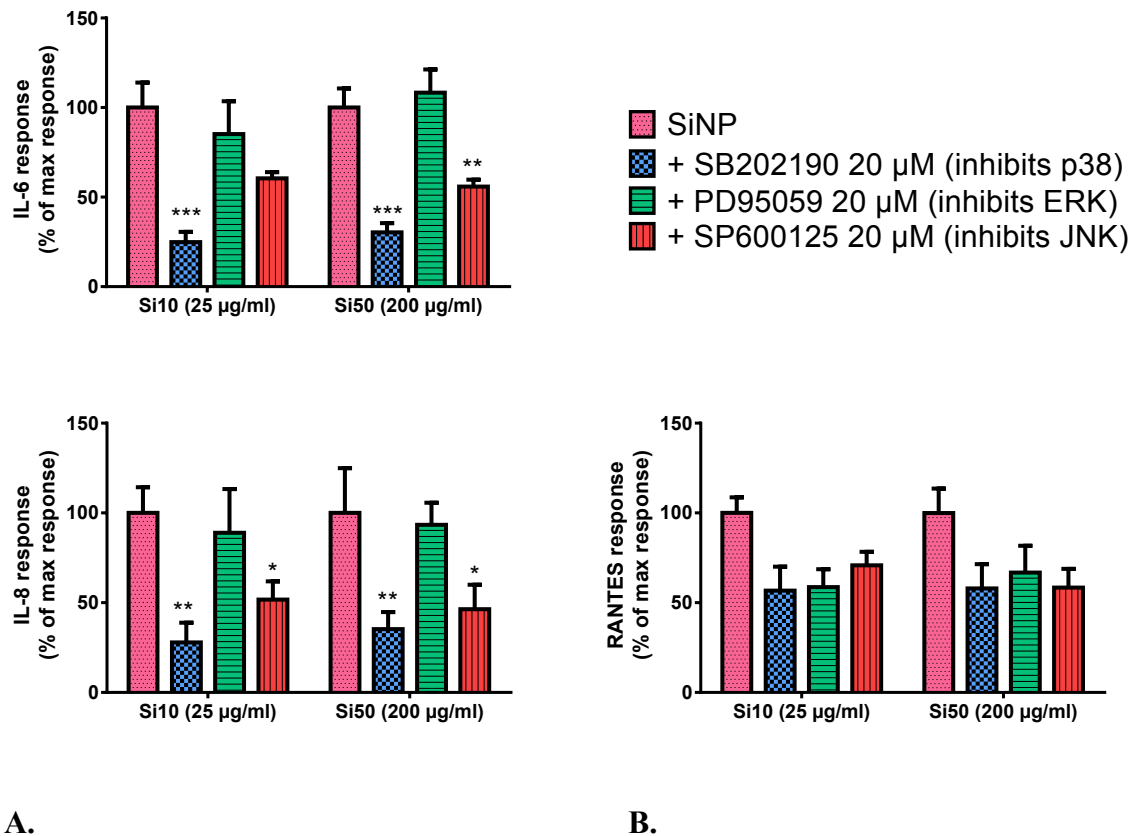


Figure 17. The involvement of MAPKs in cytokine release after exposure to Si10 and Si50. The BEAS-2B cells were exposed to Si10 (25 µg/ml) and Si50 (200 µg/ml) for 20 hours after pre-incubation with chemical inhibitors (SB202190, PD95059 and SP600125, 20 µM) of the MAPKs p38, ERK and JNK for 1 hour. The release of the cytokines was measured by ELISA as described. The results are shown as percentage release of maximal response. Max IL-6 responses of Si10 and Si50 were 21100 and 20736 pg/ml, respectively. Max IL-8 responses of Si10 and Si50 were 12679 and 10523 pg/ml, respectively. Max RANTES responses of Si10 and Si50 were 163 and 25 pg/ml, respectively. The data represents mean ± SEM from at least 4 experiments. * $p < 0.05$, ** $p < 0.01$, *** $p < 0.001$ for Dunnett's one-way ANOVA.

A. The release of IL-6 and IL-8. B. The release of RANTES.

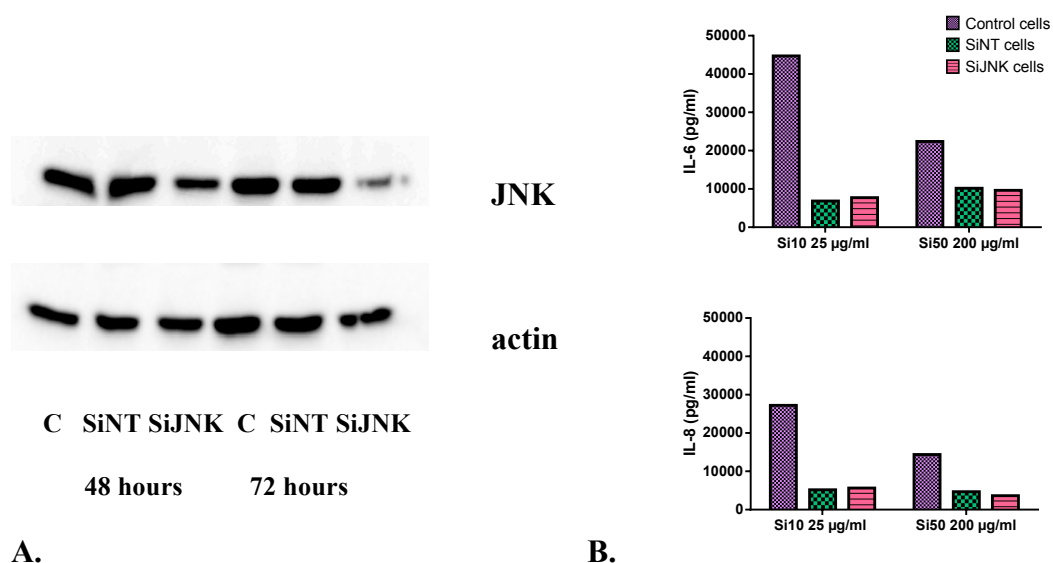


Figure 18. Effect of siRNA against JNK on cytokine release induced by Si10 and Si50.

The cells were transfected with a mixture of HiPerfect/SiNT or HiPerfect/SiJNK2 (6µl/10nmol) in LHC-9 medium the same day of the cell-plating, removed after 24 hours and replaced with DMEM/F-12 medium. The cell were exposed to 25 µg/ml Si10 and 200 µg/ml Si50 after 48 hours, and the supernatants harvested after 72 hours and analysed with ELISA as described. The results shown are from one experiment. Control cells were taken at 48 hours and 72 hours to assess the transfection efficiency.

A. Western blot of transfection efficiency.

B. IL-6 and IL-8 release

4.4.2 The involvement of TGF-α/EGFR pathway on the cytokine release

EGFR regulates many processes due to its ability to activate different signalling proteins. TGF-α is an important activating ligand of EGFR. In this study, the TGF-α release after exposure to Si10 and SI50 were investigated. The inhibition of ectodomain shedding of proTGF-α and phosphorylation of EGFR with respect to the cytokine release were also studied. The ecodomain shedding of proTGF-α was assessed by inhibiting the endoproteolytic enzyme, TACE, while EGFR phosphorylation was inhibited by a chemical reagent.

4.4.2.1 Inhibition of EGFR and TACE

The BEAS-2B cells were pre-treated with chemical inhibitors of the EGFR (AG1478, 10 μ M) and TACE (TAPI-1, 20 μ M) 1 hour prior to Si10 (25 μ g/ml) and Si50 (200 μ g/ml) exposure for 20 hours. The release of IL-6, IL-8 and RANTES was then analysed by ELISA. As shown in figure 19, the inhibitor of EGFR (AG1478) significantly reduced the release of all cytokines. However, the effect on RANTES after Si50 exposure was not significant. The reduction of IL-6 and IL-8 levels upon inhibiting TACE was not significant, whereas the RANTES levels seemed to be increased. Thus, EGFR, and to a less extent TACE, seems to be involved in the synthesis and release of the three cytokines IL-6, IL-8 and RANTES, as the cytokine release upon EGFR inhibition was reduced with at least 55% compared to maximal response.

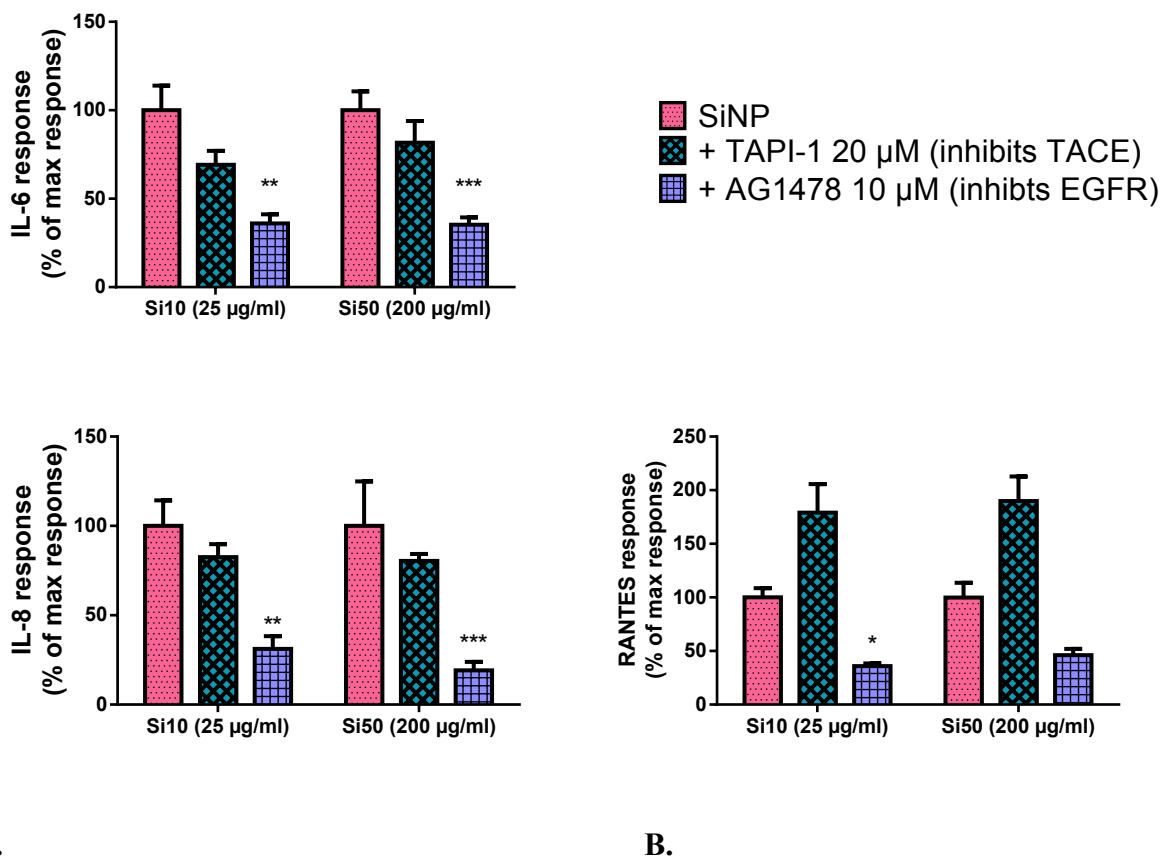


Figure 19. The involvement of EGFR and TACE in cytokine release after exposure to Si10 and Si50.

The BEAS-2B cells were exposed to Si10 (25 μ g/ml) and Si50 (200 μ g/ml) for 20 hours after pre-incubation with chemical inhibitors (TAPI-1, 20 μ M and AG1478, 10 μ M) of TACE and

EGFR for 1 hour. The release of the cytokines was measured by ELISA as described. The results are shown as percentage release of maximal response. Max IL-6 responses of Si10 and Si50 were 21100 and 20736 pg/ml, respectively. Max IL-8 responses of Si10 and Si50 were 12679 and 10523 pg/ml, respectively. Max RANTES responses of Si10 and Si50 were 163 and 25 pg/ml, respectively. Results represent mean \pm SEM from at least 4 experiments. * p <0.05, ** p <0.01, *** p <0.001 for Dunnett's one-way ANOVA.

A. The release of IL-6 and IL-8. B. The release of RANTES.

4.4.2.2 Release of TGF- α

The levels of SiNP-induced TGF- α release were assessed after exposure to Si10 (25 μ g/ml) and Si50 (200 μ g/ml) for 0.5-4 hours (figure 20). There seems to be an early release of TGF- α already after 30 minutes of particle exposure. The release seemed to be at about the same levels for at least another 3.5 hours.

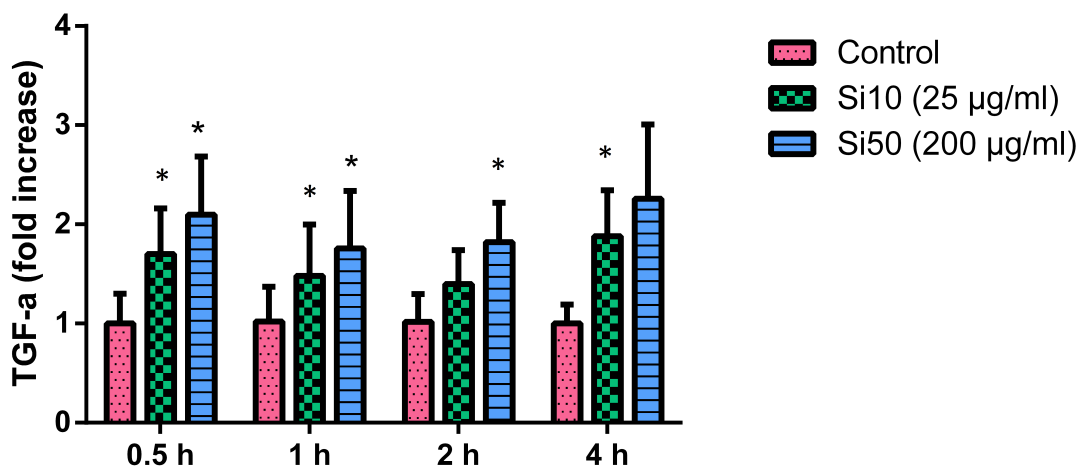


Figure 20. TGF- α release after exposure to Si10 and Si50

The cells were pre-incubated with anti-EGFR (4 μ g/ml) 30 minutes prior to exposure to 25 μ g/ml Si10 and 200 μ g/ml Si50. The supernatants were harvested at 0.5-, 1-, 2- and 4 hours and analysed with sandwich ELISA as described. The release of TGF- α is shown as fold increase of the control level. Mean controls were 3.9 pg/ml, 5.1 pg/ml, 9.0 pg/ml and 13.4 pg/ml for 0.5-, 1-, 2- and 4 hours, respectively. Results represent mean \pm SEM from 5 experiments. * p <0.05 for Holm-Sidak's one-way ANOVA.

5 Discussion

In the present thesis, pro-inflammatory responses to SiNPs of different sizes have been studied in bronchial epithelial cells with special emphasis on signalling mechanisms. Furthermore, the particles have been characterized using the relevant exposure conditions. The particle characterization revealed that Si10 and Si12 were agglomerated in the medium (DMEM/F-12), whereas Si50 did not agglomerate. Particle charge measurements indicated a large negative zeta potential ($>-30\text{mV}$) for all three particles.

All the three silica nanoparticles induced concentration-dependent pro-inflammatory responses with increased release of IL-6 and IL-8 upon reduced particle size. Notably, the responses of Si10 were markedly higher than Si12 in spite of the small size difference. For RANTES release, the responses were lower and the difference between Si12 and Si50 were less distinct. LDH release also indicated a size-dependent cytotoxicity. The studies of signalling pathways suggest the involvement of MAPKs p38 and JNK and the TGF- α /EGFR-pathway in the induction of cytokine release.

5.1 Particle characterization

Particle size. The number distributions of Si10 measurements show that the majority of the particles were around 10 nm in size when dispersed in DMEM/F-12 medium (see number distribution of Si10 in figure 12, right panel). The measurements of Si10 showed some inconsistencies between the parallel samples (see section 3.5.3). Compared to Si10, the results from Si12 measurements are consistent between the three individual samples. The results indicated, however, the existence of only large agglomerates ($> 200\text{ nm}$) and that incubation at $37\text{ }^{\circ}\text{C}$ for 2 hours further increased the particle size. This indicates that Si12 particles agglomerate in DMEM/F-12, and that the agglomeration process may continue with slow kinetics that was detected after 2 hours. Temperature may also be a contributing factor, in which increase in size due to the change of temperature has been shown to affect the kinetics of protein adsorption to particle surface [24]. If the particles are, in fact, sensitive to

temperature fluctuations, the DLS-analysed particles may not be the same as the cell-exposed particles. This may be a reason why the Si12 still induced higher pro-inflammatory responses compared to Si50. Si50 seemed to be the most stable particle of all three SiNPs. The slight reduction of z-average after 2 hours proves that the declared size of 50 nm may not be exactly true. If there is a BSA-coating around the particles, the true particle size of Si50 is even smaller than the measured value.

The results from the DLS measurements of Si10 and Si12 raise two concerns. First is the fact that the particle solutions are not stable in either water or DMEM/F-12. The other is the presence of particle agglomerates in the systems. The instability of the particles in both water and DMEM/F-12 is unwanted in studies of nanoparticles in which particle characteristics are of particular importance. An unstable particle solution give rise to an unpredictable system, making it hard to know which properties our nanoparticles inherits at all time. Since the biological effects are thought to be dependent of the particle properties, the sensitivity of SiNPs to environmental changes makes it challenging to understand cellular effects of the nanoparticles. Nanoparticles are known to bind different proteins in the biological medium that might be crucial for the agglomeration state, cellular uptake and the biological reactivity of the particles [20].

Particle charge. Particle charge is another nanoparticle characteristic that should be measured. As mentioned earlier, a particle solution with a zeta potential higher or lower than $\pm 30\text{mV}$ is in practice stable with monodispersed particles due to electrostatic forces preventing close contact. It is therefore somehow unexplainable that Si10 and Si12 still seem to agglomerate. One factor that might be of particular importance is that the zeta potential measurements are done in water, and not in DMEM/F-12. It is believed that the pH and electrolyte concentrations of physiological solutions do not provide a large enough zeta potential to prevent agglomeration; pure water does not give this effect. It should still be noted that the DLS measurements of Si10 and Si12 in water indicated agglomerated dispersions (see Appendix 3). The concluding remark is, that even though the zeta potential measurements are informative, it cannot be assumed that the particles in DMEM/F-12 have the same potential. It has, although, been found that the zeta potential for 30- and 50 nm silica

particles in LHC-9 medium was less negative [77], which might also be the case for DMEM/F-12. Nevertheless, cell medium has a high conductivity, which can lead to misguided zeta potential values [27]. This also raises the question to whether a large zeta potential is enough to give monodispersed particle solution.

There have been separate thoughts of whether positively or negatively charged particles are the most toxic; the negative cell membranes indicate a better attraction of positive particles and thereby increase particle-to-cell contact [97, 98]. Another theory speculates that negative particles may cause the formation of a proton cloud around the particles, and thereby exert more toxicity [99]. None of the three nanoparticles had a positive zeta potential, and the cellular effects of the charge of SiNPs cannot be discussed here. However, the particles induce strong cellular effects, indicating that interaction between particles and cell membranes does take place.

Conclusions of particle size and charge. Si10 and Si12 agglomerated in water and DMEM/F-12 medium, whereas Si50 did not agglomerate in neither water nor medium. The analysis also indicated partly agglomeration in Si10 solution and full agglomeration in Si12 solution. Other characterization techniques should be used in addition to DLS to get a better characterization of Si10 and Si12. Even though all three particles had a large negative surface charge, the existence of agglomerates indicates that electrostatic repulsion was not enough to stabilize particle solutions.

5.2 Cytokine and LDH release related to particle properties

Particle size has been thought to be an important property of nanoparticles that induces cellular effects [1]. A large part of the particle characterization has been focusing on determining particle size. However, the results from the cytokine- and LDH releases are not reflected in the measured particle sizes (DLS) from the particle characterization. Si12 are

measured to be around 5 times the size of Si50, due to the extended agglomeration, but are still more pro-inflammatory (IL-6 and IL-8) and cytotoxic compared to Si50. And if we assume that the number distribution based on the DLS measurements of Si10 are the critical determinant, i.e. that the size of Si10 seem to be around 10 nm, the difference in the cytokine levels induced by the three particles does not support that particle DLS-size is the determinant factor. Our results therefore suggest that the size of primary particles (as measured TEM) by the manufacturer) and/or other particle properties may be responsible for the toxic effects of SiNPs.

5.2.1 Particle size – is it really the determinant factor?

Even though particle size is believed to be an important property of biological effects, other characteristics may also be of importance, for example shape, morphology, crystallinity, composition, surface chemistry and surface area [8]. This assumption is supported by Fruijtier-Pölloth who states that biological activity of synthetic amorphous silica is related to particle shape and surface characteristics rather than particle size [92]. Si50 retained the size of around 50 nm, and it is therefore thought that Si50 retain its spherical shape in both water and DMEM/F-12. The same measurements of Si10 and Si12 indicated presence of agglomerates – some agglomeration in Si10 solution whereas complete agglomeration of Si12 particles. The agglomerates are therefore believed to deviate from the spherical shape of the primary particles. The agglomerates do, on the other hand, still possess approximately the same total surface area as the sum of surface areas of the individual particles due to pits and gaps between agglomerated particles [92]. It therefore seems as if surface area, rather than particle size, is the influencing factor of biological effects in the present study. This assumption is supported by Rabolli et al. which demonstrated that cytotoxic activity of amorphous silica nanoparticles is mainly influenced by surface area and not by aggregation state [100]. Napierska et al. also imply that surface area is an important determinant factor for the cytotoxic properties of silica nanoparticles [101]. The same assumption was made by Passagne et al. which believe that the increased surface area give rise to better interaction with cell membrane [88]. In addition, particles of 10 nm in size have approximately twice the number of atoms on their surface compared to particles larger than 30 nm [102].

For the nanoparticles to induce biological effects, they need to come in contact with the cells at the bottom. Teeguarden et al. believe that sedimentation is the main force leading to the contact of particles to the cells at the bottom of a well during exposure [17]. Agglomeration state is therefore assumed to be an important factor contributing to cellular effects due to the increase in size, and thereby are subject of the gravitational force. They estimated only a small fraction of non-agglomerated particles to reach the cells. The latter assumption does not apply in our study due to the demonstrated SiNP-induced responses as early as 0.5 hour. In contrary to Teeguarden et al., Lison et al. do not believe in that agglomeration affect cellular responses to such a large extent [13]. There is a difference between which size cut-off is postponed to sedimentation due to difference in density etc. It is previously mentioned that particles in nanometer range are not subject to sedimentation, but rather come in contact with cells through Brownian motion. It is described that particles in range of 150-500 nm can sediment [16, 92]. Sedimentation may enable agglomerates of Si10 and Si12 to more efficiently come in contact with cells at a faster rate and higher dose compared to Si50, and might also be a possible explanation for the difference in the toxicity between Si10, Si12 and Si50. In this study, it seems as both models of Teeguarden et al and Lison et al. have an impact, since nano-sized Si50, which are less prone to sedimentation, are able to induce cellular responses. It should be noted that, even if agglomeration does not affect the total surface area and hence biological effects, the increased sedimentation rate enable more particles/surfaces, i.e. larger effective dose, to come in contact with cells and thereby exert their effects. This might explain the larger pro-inflammatory potential of silica nanoparticle of 500 nm compared to 50 nm found in our previous study [71].

The theoretic calculations (section 3.5.2) imply a larger surface area exposure of the applied concentrations of Si50 compared to Si10. However, SiNP-induced cytokine release indicated that Si10 were more pro-inflammatory than Si50. Due to the differences in both cytokine- and LDH levels of the two particles, this indicate that surface area alone is not the cause of the silica particles' pro-inflammatory potential, and that there are other properties and processes that contribute to the toxic effects. However, it is important to have in mind that this is only a theoretical approximation; the conditions for these to be true numbers are monodispersity and

that all particles reach the cells during exposure. Based on the DLS measurements, the latter is not true for, at least, Si10.

An additional particle property that may influence pro-inflammatory effects is surface reactivity. In our study on rhodamine-coated- and plain silica particles, the rhodamine particles induced more effects [71]. The particle characterization, however, indicated similar particle size between plain and coated particles. This indicates that surface chemistry probably also plays a role in addition to surface area. This might be due to the rhodamine-residues *per se* or a higher density of active residues (OH groups or others) per surface unit. The same study also found that agglomerated particles (in absence of BSA) were more toxic than BSA-coated, monodispersed particles; this difference is believed to be due to reduced surface reactivity upon protein adsorption [77].

Studying the cell cytotoxicity also helps understanding some part of the pattern of cytokine release. The highest concentrations of Si10 and Si12 gave a reduced cytokine release. A logical explanation of this is that high cell cytotoxicity occurs at these concentrations. In addition, less difference was observed for LDH release than for IL-6 and IL-8 release when comparing Si10 and Si12. This might imply that, whereas cytotoxicity (LDH release) is largely affected by particle size, there might be other factors in addition to particle size that stimulates cytokine release.

Several studies have identified different mechanisms that can eventually lead to cell death. Processes of ROS, destruction of membrane integrity, cell lysis and induction of apoptosis have all proven to be initiated by silica nanoparticles [83-90, 93, 103, 104]. A combination of all these processes might therefore result to the cytotoxicity of silica particles, and different activation of these mechanisms might contribute to the different cytotoxicity between different sizes of same material. When ROS is dominating, the extent of activation of antioxidant systems is also believed to play a major role in cell survival. The difference between the particles cytotoxic potential can be due to the activation of different processes to a different extent. The size-dependent cytotoxicity observed in the present study is also

supported by others [88, 101, 105]. On the other side, many studies with several cell lines do not support this [81, 106, 107]. Whether there is a size-dependent cytotoxicity of silica nanoparticles is therefore still unclear, and should be further assessed; these contradictory results indicate, however, that other factors in addition to particle size might influence.

In conclusion, the induction of all three SiNPs in the release of IL-6, IL-8 and RANTES was only partly dependent on particle size. However, the smaller the particle size, the higher the levels of cytokine release. Our data suggest that other properties such as surface area (reflecting the size measured by TEM), and not the DLS-size, may play a major role. Agglomerates may, however, be subject to gravitational forces enabling a large effective dose to reach the cells. Thus, there is a possibility that the differences between the SiNPs, at least partly, are attributed to this particular force. Furthermore, our data do not support a role of particle charge in inducing cellular responses.

5.3 Signalling pathways involved in the cytokine release

We have previously shown that activation of MAPKs and TGF- α and EGFR is involved in the induction of IL-8 and IL-6 [60, 79]. This was also observed in BEAS-2B-exposed Si50 cultures [76]. MAPKs p38 and JNK have been shown to regulate RANTES induced by other stress responses in bronchial epithelial cells [108]. In the present study, Si10 induced higher cytokine levels than Si50. Furthermore, the MAPKs seemed to be similarly involved for Si10 as observed for Si50. Thus, there might also be other signal mechanisms involved that are responsible for the high Si10 cytokine levels. It has been stated that the IL-8 promoter has three seats for three different transcription factors, C/EBP, NF- κ B and AP-1 [38, 44, 65], and that all three need to be bound for maximum IL-8 transcription. These proteins have not been studied here, but it has previously been shown that Si50 activates NF- κ B [76]. A difference in the particles ability to activate the transcription factors may be a reason for the difference in their pro-inflammatory potential.

The present study shows that both Si10 and Si50 mediate the IL-6 and IL-8 responses via p38 and JNK signalling pathways. This is demonstrated by phosphorylation patterns of these MAPKs as well as experiments with chemical inhibitors of the respective MAPKs. Even though the results from siRNA against JNK showed no involvement of JNK in mediating cytokine release, the other two experiments were done more extensive and thorough with convincing JNK-involvement. Our previous study of Si50 did not demonstrate a role for JNK in the cytokine induction in BEAS-2B cells, although JNK was strongly phosphorylated [76]. The explanation of this discrepancy is unclear, but could be due to difference in antibody used or cell passage number of the BEAS-2B cells.

In this study, the inhibition of ERK did not give reduced cytokine levels, but there was a slightly increased phosphorylation of ERK induced by Si10 and Si50. This is in accordance to our previous study [76]. Other studies have indicated the involvement of all three MAPKs in IL-8/IL-6 transcription [60, 79]. These variable results indicate that IL-6 and IL-8 might be regulated by all three MAPKs, but that their activation may be cell type- and/or stimulants-specific. Even though ERK has seen to be activated by environmental stresses in some cases [42, 43], our results indicate that p38 and JNK are still the major stress-activated MAPKs. The role of ERK in IL-6 and IL-8 synthesis has been proven by several studies [44, 69, 109]. However, there is a possibility that a stronger activation of ERK is necessary to induce IL-6 and IL-8 transcription or that activation is cell-specific. Further studies should be done to clarify ERKs role.

As mentioned earlier, ERK is mostly known activated by mitogens such as EGF through EGFR. There has also previously been shown that the EGFR pathway leads to activation of ERK [46, 47, 54]. Furthermore, we observed that inhibition of EGFR gives a significant reduction of cytokine release, which indicate that EGFR is activated by SiNPs and involved in mediating pro-inflammatory responses. EGFR-activation was also shown in an earlier study of Si50 [76]. ERK should, even if not directly activated by SiNP, be secondary activated by EGFR. But as mention earlier, EGFR-dependent activation of ERK is regulated through

negative feedback. Since the result from Western analysis concerning ERK was diffuse and did not show a major phosphorylation upon particle exposure, there is a possibility that ERK was not directly activated by Si10 and Si50, but rather indirectly through EGFR.

In contrast to IL-6 and IL-8, RANTES release due to Si10 and Si50 exposure might involve ERK in addition to p38 and JNK. Experiments with chemical inhibitors indicated the involvement of all three MAPKs. This is different to what Furuichi et al. showed, where only p38 and JNK were demonstrated to mediate RANTES release in bronchial epithelial cells [108]. The difference here might be cell type- and/or stimulants specific. In the present study, the reduction of the RANTES levels with the MAPKs inhibitors was minor and non-significant. This might imply that other signal mechanisms may have a larger involvement in inducing RANTES transcription. SiNP-induced RANTES release showed, in addition, to be dependent on EGFR, but not TACE.

The TGF- α /EGFR-pathway has been previously demonstrated to be activated by Si50 [76]. Even though our results show negligible reduction of IL-6 and IL-8 levels and no reduction of RANTES levels when inhibiting TACE, there is still some scepticism about whether or not this is an accurate result. It has previously been shown that exposure of Si50 to BEAS-2B cells leads to reduced IL-6 and IL-8 levels when inhibiting TACE [76], which is contradictory to these results. The explanation for this discrepancy might be difference in cell passage of BEAS-2B cells used and/or TAPI-1 quality. To clarify this, further investigations to define the true role of TACE are needed. The assumption that TACE most likely is involved in SiNP-mediated activation of cytokine synthesis is supported by the increase of TGF- α release in cells exposed to Si10 and Si50. An alternative possibility that explains the increased TGF- α levels is that cleavage of proTGF- α was through a TACE-independent mechanism. As mentioned earlier, studies have shown the existence of other ADAMs that are able to cleave proTGF- α [55, 58].

Eom and Choi [82] demonstrated some results regarding signalling pathways that contradict the results from this and an earlier study [76]. They found no activation of NF- κ B, JNK or

p38, but strong activation of ERK when exposing BEAS-2B cells to porous silica particles. Since the same cell line as in the present study is used, the difference might be confined to the silica particles. The silica particles they used have a high surface area; our particles, in the other hand, are non-porous. The difference in pathways activation might therefore be due to surface area and/or surface characteristics. Kang and Lim showed that silica particles induced TNF- α production, but not IL-6 [81]. As mentioned earlier, IL-8 production has shown to be mediated through a TNF- α -dependent manner [44]. It seemed like the production of IL-6 was not regulated by this mechanism. In this paper, the involvement of ERK and p38, but not JNK was shown. This was not the case in our study though, where the inhibition studies clearly showed the involvement of JNK and p38 in the release of IL-6 and IL-8.

One other factor that also needs to be considered is the interplay between different signalling pathways. There is a possibility that the signalling proteins were indirectly activated by the particles. Cytokines are, for instance, known to activate MAPKs. There is therefore a possibility that the particles can induce cytokine release through other mechanisms, and that these cytokines again binds to membrane receptors that activate MAPKs. Cytokine-activated MAPKs can then lead to the stimulation of IL-6, IL-8- and RANTES transcription [44, 69, 109]. In addition, both EGFR and MAPKs have been shown to activate each other, and two of the MAPKs can induce ectodomain shedding of proTGF- α (section 1.5.3). This raises questions to whether the silica nanoparticles, in fact, activate the different signalling pathways directly. There is therefore a possibility that induction of cytokine transcription by SiNPs can be through secondary activation or a combination of both direct and indirect mechanisms. As different pathways may interact, our conclusions based on our results are only indicative and not definite. Wang et al. demonstrated that a pathological bacteria can induce the hosts' immune system, leading to the release of inflammatory mediators such as cytokines, and that these synergistically enhance the response. These stimulators can, together, activate multiple receptors and signalling pathways, leading to maximal activation of transcription factors and thereby maximal transcription of certain genes [50].

It should also be kept in mind that there was not found much literature studying the involvement of EGFR in silica nanoparticle-induced toxicity. The strong interaction of

MAPKs with EGFR, in addition to our results, illustrate that EGFR do have a central role, and its involvement should be studied further. Interesting activation of the EGFR has been found to be important in regulation of immunity and during different diseases conditions, including chronic obstructive pulmonary disease [54].

In conclusion, MAPKs p38 and JNK, but not ERK, were partly involved in the SiNP-induced cytokine release in BEAS-2B cells. Which MAPKs that are involved might, however, be stimulant- and cell specific. EGFR also seemed to contribute, and is most likely activated by TGF- α . However, there is still a question of whether these signalling mechanisms are directly or indirectly activated by the particles. Another interesting aspect comes from the inhibition experiments. Even though there is a clear difference in the toxicity of Si10 and Si50, their pro-inflammatory potential with the release of cytokines seemed to be mediated by the same pathways, but to somewhat different extent.

5.4 *In vivo* extrapolation

It is often used in *in vitro* models to understand cellular mechanisms and effects. However, as it has been demonstrated in the above sections, nanoparticles are sensitive objects whose properties easily alter according to the environmental changes. This also means that the results from an *in vitro* study are difficult to extrapolate to *in vivo* situations. Since this field is mainly interested in biological side effects of nanoparticles, the high sensitivity of nanomaterials questions the authenticity of the results from artificial biological cell culture systems. The biological environment in the lungs is quite different from a typical cell culture medium. In addition, Mahmoudi et al. showed that *in vivo* temperature fluctuations, i.e. 37-41 °C, affected the protein corona formation and composition significantly [24]. And as mentioned earlier, protein corona affects the properties of nanoparticles to a large extent. Thus, extrapolation from *in vitro* to *in vivo* represents challenges in investigation of adverse health effects of nanoparticles in general.

6 Conclusions

Based on the results from the present study, the following conclusions can be made:

- The magnitude of SiNP-induced IL-6 and IL-8 release was relative similar for the same particle size, with the order of potency Si10>>Si12>Si50, when related to the mass of the nanoparticles. The SiNP-induced RANTES release was less pronounced with an order of Si10>>Si12=Si50.
- The cytotoxicity of SiNPs, measured as release of LDH, showed concentration-dependent effects with an order of potency Si10>Si12>>Si50.
- With respect to signalling mechanisms, the IL-6 and IL-8 release induced by Si10 and Si50 were partly mediated by MAPKs p38 and JNK. Furthermore, EGFR-inhibition revealed that the EGFRs were involved in mediating IL-6 and IL-8 release. Both Si10 and Si50 increased the release of TGF- α , and SiNPs might be mediated by the TGF- α /EGFR-pathway. However, the role of TACE activation and TGF- α release in SiNP-induced IL-6 and IL-8 responses needs to be further clarified.
- The RANTES release may indicate a role of EGFR and MAPKs p38, JNK and ERK for both Si10 and Si50, but all these data were not significant. Similar signalling pathways seem to be involved in cytokine responses of Si10 and Si50, but to different extent.
- With respect to particle characterization, the comparison of Si10- and Si50-induced cytokine responses, when related to the surface area (estimated), indicate that this might be an important property. However, particle characterization also indicated that other parameters in addition to particle size might be important for the SiNPs pro-inflammatory and cytotoxic potentials.

7 References

1. Oberdorster, G., E. Oberdorster, and J. Oberdorster, *Nanotoxicology: an emerging discipline evolving from studies of ultrafine particles*. Environ Health Perspect, 2005. **113**(7): p. 823-39.
2. Pope, C.A., 3rd, D.V. Bates, and M.E. Raizenne, *Health effects of particulate air pollution: time for reassessment?* Environ Health Perspect, 1995. **103**(5): p. 472-80.
3. Dockery, D.W., et al., *An Association between Air Pollution and Mortality in Six U.S. Cities*. New England Journal of Medicine, 1993. **329**(24): p. 1753-1759.
4. Byrne, J.D. and J.A. Baugh, *The significance of nanoparticles in particle-induced pulmonary fibrosis*. McGill J Med, 2008. **11**(1): p. 43-50.
5. Colvin, V.L., *The potential environmental impact of engineered nanomaterials*. Nat Biotechnol, 2003. **21**(10): p. 1166-70.
6. Bihari, P., et al., *Optimized dispersion of nanoparticles for biological in vitro and in vivo studies*. Part Fibre Toxicol, 2008. **5**: p. 14.
7. Lewinski, N., V. Colvin, and R. Drezek, *Cytotoxicity of nanoparticles*. Small, 2008. **4**(1): p. 26-49.
8. Vippola, M., et al., *Preparation of nanoparticle dispersions for in-vitro toxicity testing*. Hum Exp Toxicol, 2009. **28**(6-7): p. 377-85.
9. De Jong, W.H. and P.J. Borm, *Drug delivery and nanoparticles: applications and hazards*. Int J Nanomedicine, 2008. **3**(2): p. 133-49.
10. Alkilany, A. and C. Murphy, *Toxicity and cellular uptake of gold nanoparticles: what we have learned so far?* Journal of Nanoparticle Research, 2010. **12**(7): p. 2313-2333.
11. Society, T.R., *Nanoscience and nanotechnologies: opportunities and uncertainties*. 2004.
12. de Villiers, M.M., P. Aramwit, and G.S. Kwon, *Nanotechnology in Drug Delivery*. 2008: Springer.
13. Lison, D., et al., *Nominal and effective dosimetry of silica nanoparticles in cytotoxicity assays*. Toxicol Sci, 2008. **104**(1): p. 155-62.
14. Dobrovolskaia, M.A. and S.E. McNeil, *Immunological properties of engineered nanomaterials*. Nat Nanotechnol, 2007. **2**(8): p. 469-78.
15. Boverhof, D.R. and R.M. David, *Nanomaterial characterization: considerations and needs for hazard assessment and safety evaluation*. Anal Bioanal Chem, 2010. **396**(3): p. 953-61.
16. Aulton, M.E., *Aulton's Pharmaceutics: The Design And Manufacture of Medicines*. 2007: Churchill Livingstone/Elsevier.
17. Teeguarden, J.G., et al., *Particokinetics in vitro: dosimetry considerations for in vitro nanoparticle toxicity assessments*. Toxicol Sci, 2007. **95**(2): p. 300-12.
18. Florence, A.T. and D. Attwood, *Physicochemical Principles of Pharmacy*. 2006: Pharmaceutical Press.
19. Lundqvist, M., et al., *Nanoparticle size and surface properties determine the protein corona with possible implications for biological impacts*. Proc Natl Acad Sci U S A, 2008. **105**(38): p. 14265-70.
20. Lynch, I., et al., *The nanoparticle-protein complex as a biological entity; a complex fluids and surface science challenge for the 21st century*. Adv Colloid Interface Sci, 2007. **134-135**: p. 167-74.
21. Rahman, M., et al., *Nanoparticle and Protein Corona*, in *Protein-Nanoparticle Interactions*. 2013, Springer Berlin Heidelberg. p. 21-44.

22. Tenzer, S., et al., *Rapid formation of plasma protein corona critically affects nanoparticle pathophysiology*. Nat Nanotechnol, 2013. **8**(10): p. 772-81.
23. Maiorano, G., et al., *Effects of cell culture media on the dynamic formation of protein-nanoparticle complexes and influence on the cellular response*. ACS Nano, 2010. **4**(12): p. 7481-91.
24. Mahmoudi, M., et al., *Temperature: the "ignored" factor at the NanoBio interface*. ACS Nano, 2013. **7**(8): p. 6555-62.
25. Buford, M., R. Hamilton, and A. Holian, *A comparison of dispersing media for various engineered carbon nanoparticles*. Particle and Fibre Toxicology, 2007. **4**(1): p. 6.
26. Deguchi, S., et al., *Stabilization of C60 nanoparticles by protein adsorption and its implications for toxicity studies*. Chem Res Toxicol, 2007. **20**(6): p. 854-8.
27. Murdock, R.C., et al., *Characterization of nanomaterial dispersion in solution prior to in vitro exposure using dynamic light scattering technique*. Toxicol Sci, 2008. **101**(2): p. 239-53.
28. Mandzy, N., E. Grulke, and T. Druffel, *Breakage of TiO₂ agglomerates in electrostatically stabilized aqueous dispersions*. Powder Technology, 2005. **160**(2): p. 121-126.
29. Hillery, A.M., A.W. Lloyd, and J. Swarbrick, *Drug Delivery and Targeting: For Pharmacists and Pharmaceutical Scientists*. 2003: Taylor & Francis.
30. Jud, C., et al., *Nanomaterials and the human lung: what is known and what must be deciphered to realise their potential advantages?* Swiss Med Wkly, 2013. **143**: p. w13758.
31. Scheuch, G. and R. Siekmeier, *Novel approaches to enhance pulmonary delivery of proteins and peptides*. J Physiol Pharmacol, 2007. **58 Suppl 5**(Pt 2): p. 615-25.
32. Seaton, A., et al., *Particulate air pollution and acute health effects*. Lancet, 1995. **345**(8943): p. 176-8.
33. Pope, C.A., 3rd, et al., *Heart rate variability associated with particulate air pollution*. Am Heart J, 1999. **138**(5 Pt 1): p. 890-9.
34. Nemmar, A., et al., *Passage of inhaled particles into the blood circulation in humans*. Circulation, 2002. **105**(4): p. 411-4.
35. Takenaka, S., et al., *Pulmonary and systemic distribution of inhaled ultrafine silver particles in rats*. Environ Health Perspect, 2001. **109 Suppl 4**: p. 547-51.
36. Elder, A.C., et al., *Systemic effects of inhaled ultrafine particles in two compromised, aged rat strains*. Inhal Toxicol, 2004. **16**(6-7): p. 461-71.
37. Heinrich, P.C., et al., *Principles of interleukin (IL)-6-type cytokine signalling and its regulation*. Biochem J, 2003. **374**(Pt 1): p. 1-20.
38. Holtmann, H., et al., *Induction of interleukin-8 synthesis integrates effects on transcription and mRNA degradation from at least three different cytokine- or stress-activated signal transduction pathways*. Mol Cell Biol, 1999. **19**(10): p. 6742-53.
39. Matsukura, S., et al., *Expression of IL-6, IL-8, and RANTES on human bronchial epithelial cells, NCI-H292, induced by influenza virus A*. J Allergy Clin Immunol, 1996. **98**(6 Pt 1): p. 1080-7.
40. Kaminska, B., *MAPK signalling pathways as molecular targets for anti-inflammatory therapy--from molecular mechanisms to therapeutic benefits*. Biochim Biophys Acta, 2005. **1754**(1-2): p. 253-62.
41. Kyriakis, J.M. and J. Avruch, *Mammalian mitogen-activated protein kinase signal transduction pathways activated by stress and inflammation*. Physiol Rev, 2001. **81**(2): p. 807-69.

42. Kyriakis, J.M. and J. Avruch, *Mammalian MAPK signal transduction pathways activated by stress and inflammation: a 10-year update*. *Physiol Rev*, 2012. **92**(2): p. 689-737.
43. Cargnello, M. and P.P. Roux, *Activation and function of the MAPKs and their substrates, the MAPK-activated protein kinases*. *Microbiol Mol Biol Rev*, 2011. **75**(1): p. 50-83.
44. Hoffmann, E., et al., *Multiple control of interleukin-8 gene expression*. *J Leukoc Biol*, 2002. **72**(5): p. 847-55.
45. Fischer, O.M., et al., *Oxidative and osmotic stress signaling in tumor cells is mediated by ADAM proteases and heparin-binding epidermal growth factor*. *Mol Cell Biol*, 2004. **24**(12): p. 5172-83.
46. Wells, A., *EGF receptor*. *The International Journal of Biochemistry & Cell Biology*, 1999. **31**(6): p. 637-643.
47. Jorissen, R.N., et al., *Epidermal growth factor receptor: mechanisms of activation and signalling*. *Experimental Cell Research*, 2003. **284**(1): p. 31-53.
48. Schneider, M.R. and E. Wolf, *The epidermal growth factor receptor ligands at a glance*. *J Cell Physiol*, 2009. **218**(3): p. 460-6.
49. Watanabe, T., et al., *Synergistic activation of NF-kappaB by nontypeable Haemophilus influenzae and tumor necrosis factor alpha*. *Proc Natl Acad Sci U S A*, 2004. **101**(10): p. 3563-8.
50. Wang, W.Y., J.H. Lim, and J.D. Li, *Synergistic and feedback signaling mechanisms in the regulation of inflammation in respiratory infections*. *Cell Mol Immunol*, 2012. **9**(2): p. 131-5.
51. Xu, X., et al., *Activation of epidermal growth factor receptor is required for NTHi-induced NF-kappaB-dependent inflammation*. *PLoS One*, 2011. **6**(11): p. e28216.
52. Xu, K. and H.K. Shu, *EGFR activation results in enhanced cyclooxygenase-2 expression through p38 mitogen-activated protein kinase-dependent activation of the Sp1/Sp3 transcription factors in human gliomas*. *Cancer Res*, 2007. **67**(13): p. 6121-9.
53. Liu, K., et al., *Epidermal growth factor receptor signaling to Erk1/2 and STATs control the intensity of the epithelial inflammatory responses to rhinovirus infection*. *J Biol Chem*, 2008. **283**(15): p. 9977-85.
54. Vallath, S., et al., *Targeting EGFR signalling in chronic lung disease: therapeutic challenges and opportunities*. *Eur Respir J*, 2014.
55. Hinkle, C.L., et al., *Multiple metalloproteinases process protransforming growth factor-alpha (proTGF-alpha)*. *Biochemistry*, 2003. **42**(7): p. 2127-36.
56. Harris, R.C., E. Chung, and R.J. Coffey, *EGF receptor ligands*. *Exp Cell Res*, 2003. **284**(1): p. 2-13.
57. Horiuchi, K., *A brief history of tumor necrosis factor alpha--converting enzyme: an overview of ectodomain shedding*. *Keio J Med*, 2013. **62**(1): p. 29-36.
58. Merlos-Suarez, A., et al., *Metalloprotease-dependent protransforming growth factor-alpha ectodomain shedding in the absence of tumor necrosis factor-alpha-converting enzyme*. *J Biol Chem*, 2001. **276**(51): p. 48510-7.
59. Black, R.A., *Tumor necrosis factor-alpha converting enzyme*. *Int J Biochem Cell Biol*, 2002. **34**(1): p. 1-5.
60. Refsnes, M., et al., *Fluoride-induced IL-8 release in human epithelial lung cells: relationship to EGF-receptor-, SRC- and MAP-kinase activation*. *Toxicol Appl Pharmacol*, 2008. **227**(1): p. 56-67.
61. Griego, S.D., et al., *Role of p38 mitogen-activated protein kinase in rhinovirus-induced cytokine production by bronchial epithelial cells*. *J Immunol*, 2000. **165**(9): p. 5211-20.

62. Habib, A.A., et al., *The epidermal growth factor receptor engages receptor interacting protein and nuclear factor-kappa B (NF-kappa B)-inducing kinase to activate NF-kappa B. Identification of a novel receptor-tyrosine kinase signalosome.* J Biol Chem, 2001. **276**(12): p. 8865-74.
63. Schroth, M.K., et al., *Rhinovirus replication causes RANTES production in primary bronchial epithelial cells.* Am J Respir Cell Mol Biol, 1999. **20**(6): p. 1220-8.
64. Fan, H. and R. Derynck, *Ectodomain shedding of TGF-alpha and other transmembrane proteins is induced by receptor tyrosine kinase activation and MAP kinase signaling cascades.* EMBO J, 1999. **18**(24): p. 6962-72.
65. Li, J., et al., *Regulation of human airway epithelial cell IL-8 expression by MAP kinases.* Am J Physiol Lung Cell Mol Physiol, 2002. **283**(4): p. L690-9.
66. Jung, Y.D., et al., *Role of P38 MAPK, AP-1, and NF-kappaB in interleukin-1beta-induced IL-8 expression in human vascular smooth muscle cells.* Cytokine, 2002. **18**(4): p. 206-13.
67. Wu, H.M., H.C. Wen, and W.W. Lin, *Proteasome inhibitors stimulate interleukin-8 expression via Ras and apoptosis signal-regulating kinase-dependent extracellular signal-related kinase and c-Jun N-terminal kinase activation.* Am J Respir Cell Mol Biol, 2002. **27**(2): p. 234-43.
68. Kumar, A., A.J. Knox, and A.M. Boriek, *CCAAT/enhancer-binding protein and activator protein-1 transcription factors regulate the expression of interleukin-8 through the mitogen-activated protein kinase pathways in response to mechanical stretch of human airway smooth muscle cells.* J Biol Chem, 2003. **278**(21): p. 18868-76.
69. Jijon, H.B., et al., *MAP kinases contribute to IL-8 secretion by intestinal epithelial cells via a posttranscriptional mechanism.* Am J Physiol Cell Physiol, 2002. **283**(1): p. C31-41.
70. Harrison, D.A., *The Jak/STAT pathway.* Cold Spring Harb Perspect Biol, 2012. **4**(3).
71. Skuland, T., et al., *Role of size and surface area for pro-inflammatory responses to silica nanoparticles in epithelial lung cells: Importance of exposure conditions.* Toxicology in Vitro, 2014. **28**(2): p. 146-155.
72. Wang, Y., et al., *STAT3 activation in response to IL-6 is prolonged by the binding of IL-6 receptor to EGF receptor.* Proc Natl Acad Sci U S A, 2013. **110**(42): p. 16975-80.
73. Mossman, B.T. and A. Churg, *Mechanisms in the pathogenesis of asbestosis and silicosis.* Am J Respir Crit Care Med, 1998. **157**(5 Pt 1): p. 1666-80.
74. Warheit, D.B., T.A. McHugh, and M.A. Hartsky, *Differential pulmonary responses in rats inhaling crystalline, colloidal or amorphous silica dusts.* Scand J Work Environ Health, 1995. **21 Suppl 2**: p. 19-21.
75. Cho, W.S., et al., *Inflammatory mediators induced by intratracheal instillation of ultrafine amorphous silica particles.* Toxicol Lett, 2007. **175**(1-3): p. 24-33.
76. Skuland, T., et al., *Silica nanoparticles induce cytokine responses in lung epithelial cells through activation of NF-kappaB signaling and a p38/TACE/TGF-alpha/EGFR-pathway.* IN PRESS.
77. Gualtieri, M., et al., *Importance of agglomeration state and exposure conditions for uptake and pro-inflammatory responses to amorphous silica nanoparticles in bronchial epithelial cells.* Nanotoxicology, 2012. **6**(7): p. 700-712.
78. Sandberg, W.J., et al., *Comparison of non-crystalline silica nanoparticles in IL-1beta release from macrophages.* Part Fibre Toxicol, 2012. **9**: p. 32.
79. Ovreivik, J., et al., *p38 and Src-ERK1/2 pathways regulate crystalline silica-induced chemokine release in pulmonary epithelial cells.* Toxicol Sci, 2004. **81**(2): p. 480-90.

80. Val, S., et al., *Carbon black and titanium dioxide nanoparticles induce pro-inflammatory responses in bronchial epithelial cells: need for multiparametric evaluation due to adsorption artifacts*. *Inhal Toxicol*, 2009. **21 Suppl 1**: p. 115-22.
81. Kang, K. and J.S. Lim, *Induction of functional changes of dendritic cells by silica nanoparticles*. *Immune Netw*, 2012. **12**(3): p. 104-12.
82. Eom, H.J. and J. Choi, *Oxidative stress of silica nanoparticles in human bronchial epithelial cell, Beas-2B*. *Toxicol In Vitro*, 2009. **23**(7): p. 1326-32.
83. Wang, F., et al., *Oxidative mechanisms contribute to nanosize silican dioxide-induced developmental neurotoxicity in PC12 cells*. *Toxicol In Vitro*, 2011. **25**(8): p. 1548-56.
84. Napierska, D., et al., *The nanosilica hazard: another variable entity*. *Part Fibre Toxicol*, 2010. **7**(1): p. 39.
85. Ye, Y., et al., *Nano-SiO₂ induces apoptosis via activation of p53 and Bax mediated by oxidative stress in human hepatic cell line*. *Toxicol In Vitro*, 2010. **24**(3): p. 751-8.
86. Nabeshi, H., et al., *Amorphous nanosilica induce endocytosis-dependent ROS generation and DNA damage in human keratinocytes*. *Part Fibre Toxicol*, 2011. **8**: p. 1.
87. Gong, C., et al., *The role of reactive oxygen species in silicon dioxide nanoparticle-induced cytotoxicity and DNA damage in HaCaT cells*. *Mol Biol Rep*, 2012. **39**(4): p. 4915-25.
88. Passagne, I., et al., *Implication of oxidative stress in size-dependent toxicity of silica nanoparticles in kidney cells*. *Toxicology*, 2012. **299**(2-3): p. 112-24.
89. Park, E.J., et al., *Oxidative stress and apoptosis induced by titanium dioxide nanoparticles in cultured BEAS-2B cells*. *Toxicol Lett*, 2008. **180**(3): p. 222-9.
90. Wang, F., et al., *Oxidative stress contributes to silica nanoparticle-induced cytotoxicity in human embryonic kidney cells*. *Toxicol In Vitro*, 2009. **23**(5): p. 808-15.
91. L'Azou, B., et al., *In vitro effects of nanoparticles on renal cells*. *Part Fibre Toxicol*, 2008. **5**: p. 22.
92. Fruijtier-Pölloth, C., *The toxicological mode of action and the safety of synthetic amorphous silica—A nanostructured material*. *Toxicology*, 2012. **294**(2-3): p. 61-79.
93. Costantini, L.M., R.M. Gilberti, and D.A. Knecht, *The phagocytosis and toxicity of amorphous silica*. *PLoS One*, 2011. **6**(2): p. e14647.
94. Erdogdu, G. and V. Hasirci, *An overview of the role of mineral solubility in silicosis and asbestosis*. *Environ Res*, 1998. **78**(1): p. 38-42.
95. Gosens, I., et al., *Impact of agglomeration state of nano- and submicron sized gold particles on pulmonary inflammation*. *Particle and Fibre Toxicology*, 2010. **7**(1): p. 37.
96. Rahman, M., et al., *Protein-Nanoparticle Interactions: The Bio-Nano Interface*. 2013: Springer.
97. Lockman, P.R., et al., *Nanoparticle surface charges alter blood-brain barrier integrity and permeability*. *J Drug Target*, 2004. **12**(9-10): p. 635-41.
98. Oh, W.-K., et al., *Cellular Uptake, Cytotoxicity, and Innate Immune Response of Silica-Titania Hollow Nanoparticles Based on Size and Surface Functionality*. *ACS Nano*, 2010. **4**(9): p. 5301-5313.
99. Veronesi, B., et al., *The surface charge of visible particulate matter predicts biological activation in human bronchial epithelial cells*. *Toxicol Appl Pharmacol*, 2002. **178**(3): p. 144-54.
100. Rabolli, V., et al., *The cytotoxic activity of amorphous silica nanoparticles is mainly influenced by surface area and not by aggregation*. *Toxicol Lett*, 2011. **206**(2): p. 197-203.

101. Napierska, D., et al., *Size-dependent cytotoxicity of monodisperse silica nanoparticles in human endothelial cells*. *Small*, 2009. **5**(7): p. 846-53.
102. Auffan, M., et al., *Chemical stability of metallic nanoparticles: A parameter controlling their potential cellular toxicity in vitro*. *Environmental Pollution*, 2009. **157**(4): p. 1127-1133.
103. Gilberti, R.M., G.N. Joshi, and D.A. Knecht, *The phagocytosis of crystalline silica particles by macrophages*. *Am J Respir Cell Mol Biol*, 2008. **39**(5): p. 619-27.
104. Sun, L., et al., *Cytotoxicity and mitochondrial damage caused by silica nanoparticles*. *Toxicol In Vitro*, 2011. **25**(8): p. 1619-29.
105. Waters, K.M., et al., *Macrophage Responses to Silica Nanoparticles are Highly Conserved Across Particle Sizes*. *Toxicological Sciences*, 2009. **107**(2): p. 553-569.
106. Lin, W., et al., *In vitro toxicity of silica nanoparticles in human lung cancer cells*. *Toxicology and Applied Pharmacology*, 2006. **217**(3): p. 252-259.
107. Cha, K.E. and H. Myung, *Cytotoxic effects of nanoparticles assessed in vitro and in vivo*. *J Microbiol Biotechnol*, 2007. **17**(9): p. 1573-8.
108. Furuichi, S., et al., *p38 mitogen-activated protein kinase and c-Jun-NH2-terminal kinase regulate interleukin-8 and RANTES production in hyperosmolarity stimulated human bronchial epithelial cells*. *Respirology*, 2002. **7**(3): p. 193-200.
109. Vanden Berghe, W., et al., *p38 and extracellular signal-regulated kinase mitogen-activated protein kinase pathways are required for nuclear factor-kappaB p65 transactivation mediated by tumor necrosis factor*. *J Biol Chem*, 1998. **273**(6): p. 3285-90.

Appendix 1: Other materials used in the study

Kits:	Manufacturer:
Cytotoxicity Detection Kit (LDH)	Roche Diagnostics Deutschland GmbH 68305 Mannheim, Germany
DC-Protein assay	Bio-Rad Laboratories Ltd, UK
SuperSignal WestDura	Thermo Fisher Scientific Inc, Rockford, USA
Re-blot plus	CHEMICON, Millipore, Billerica, MA ,USA
TGF- α DuoSet	R&D Systems, Inc, UK
IL-8 CytoSet	Invitrogen, Life Technologies Ltd, UK
IL-6 Cytoset	Invitrogen, Life Technologies Ltd, UK

Chemical inhibitors:	Manufacturer:
SB202190	Calbiochem, Merck KGaA, Darmstadt, Germany
SP600125	Calbiochem, Merck KGaA, Darmstadt, Germany

PD95059	Calbiochem, Merck KGaA, Darmstadt, Germany
AG1478	Calbiochem, Merck KGaA, Darmstadt, Germany
TAPI-1	Calbiochem, Merck KGaA, Darmstadt, Germany

siRNA	Manufacturer:
SignalSilence siJNK siRNA	Cell Signalling Technology, Inc., Danvers, MA 01923, USA
SignalSilence Control siRNA	Cell Signalling Technology, Inc., Danvers, MA 01923, USA

Antibodies:	Manufacturer:
Anti-ERK2 (1/5000 i 3 % tørrmelk)	Santa Cruz Biotechnology, Inc. Santa Cruz, CA. U.S.A.
Anti-pERK1/2 (1/2000 i 3 % tørrmelk)	Santa Cruz Biotechnology, Inc. Santa Cruz, CA. U.S.A.
Anti-p-p38 (1/1000 i 5 % BSA)	Cell Signalling Technology, Inc., Danvers, MA 01923, USA
Anti-p-38 (1/1000 i 5 % BSA)	Cell Signalling Technology, Inc., Danvers, MA 01923, USA

Anti -JNK (1/1000 i 5 % BSA)	Cell Signalling Technology, Inc., Danvers, MA 01923, USA
Anti-p-JNK (1/1000 i 5 % BSA)	Cell Signalling Technology, Inc., Danvers, MA 01923, USA
Anti- β -Aktin (1/400.000i 3 % tørrmelk)	Sigma-Aldrich, St. Louis, MO, USA
Polyclonal Goat Anti-Rabbit Immunoglobulins/HRP	DAKO, Oslo, Norge
Polyclonal Rabbit Anti-Mouse Immunoglobulins/HRP	DAKO, Oslo, Norge

Chemicals, reagents and solutions:	Manufacturer:
Paraformaldehyde	Sigma-Aldrich, St. Louis, MO, USA
BSA (albumin, bovine)	Sigma-Aldrich, St. Louis, MO, USA
Acrylamid-eBis (37% solution)	Bio-Rad Laboratories Ltd, UK
TEMED	Bio-Rad Laboratories Ltd, UK
APS	Bio-Rad Laboratories Ltd, UK
Sodium dodecyl sulfate (SDS)	Fluka, Sigma-Aldrich, St. Louis, MO, USA
B-mercaptoethanol	Sigma-Aldrich, St. Louis, MO, USA
Glycerol	Merck, Whitehouse Station, NJ USA
Leupeptin	Sigma-Aldrich, St. Louis, MO, USA
Aprotenin	Sigma-Aldrich, St. Louis, MO, USA
Pepstatin	Sigma-Aldrich, St. Louis, MO, USA

PMFS	Sigma-Aldrich, St. Louis, MO, USA
Trizma hydrochloride	Sigma-Aldrich, St. Louis, MO, USA
Sodium chloride	Merck, Whitehouse Station, NJ USA
EDTA	Sigma-Aldrich, St. Louis, MO, USA
EGTA	Sigma-Aldrich, St. Louis, MO, USA
Sodium pyrophosphat	Sigma-Aldrich, St. Louis, MO, USA
Sodium ortovanadat	Sigma-Aldrich, St. Louis, MO, USA
Sodium flouride	Riedel-de Haën, Sigma-Aldrich, St. Louis, MO, USA
Triton X-100	Sigma-Aldrich, St. Louis, MO, USA
Dry milk	Fluka, Sigma-Aldrich, St. Louis, MO, USA
3,3',5,5'-Tetramethylbenzidine (TMB)	Merck, Whitehouse Station, NJ USA
H ₂ O ₂	Merck, Whitehouse Station, NJ USA
Trizma Base	Sigma-Aldrich, St. Louis, MO, USA
Tween 20	Sigma-Aldrich, St. Louis, MO, USA
Potassium chloride	Merck, Whitehouse Station, NJ USA
Na ₂ HPO ₄	Merck, Whitehouse Station, NJ USA
KH ₂ PO ₄	Merck, Whitehouse Station, NJ USA
HiPerfect	Qiagen GmbH, Hilden, Tyskland

Instruments:	Manufacturer:
TECAN Sunrise plate reader	TECAN Østerrike GmbH
Sonicator	Sonics & Materials, Inc. Newtown, USA
Chemi-Doc	Bio-Rad Laboratories Ltd, UK
Bioruptor	
Zetasizer Nano SZ	Malvern Instrument Ltd , United Kingdom

Equipments:	Manufacturer:
PROTEAN Nitrocellulose Transfer Membrane	Whatman GmbH, Dassel, Tyskland
Super RX Fuji medical X-ray film	FUJIFILM Corporation, Tokyo, Japan
Micro titer plate	Nunc A/S, Roskilde, Danmark
Cell culture bottles	Nunc A/S, Roskilde, Danmark
6-well plate	Corning, Lowell, MA 01851 USA
10 cm dishes	Corning, Lowell, MA 01851 USA

Appendix 2: Solutions used in the study

Solutions for Western blotting:

5 x lysisbuffer:

Tris-HCl 0.5 M pH 7.5	6 ml
Sodium chloride	1.3 g
EDTA 0.5 M	300 μ l
EGTA	57 mg
Sodium pyrophosphate	167 mg
Sodium orthovanadate	32.4 mg
Triton X-100	1500 μ l
Distilled water	ad 30 ml

1 x lysisbuffer:

5 x lysisbuffer	1 ml
10 mg/ml Aprotinin	5 μ l
1 mg/ml Pepstatin	50 μ l
10 mg/ml Leupeptin	5 μ l
0.1 M PMFS	50 μ l
Distilled water	3.935 ml

10 x electrophoresis buffer:

Trizma-base	30 g
Glycine	144 g
SDS	10 g
Distilled water	1000 ml

Diluted to 1 x electrophoresis buffer for electrophoresis

10 x transfer buffer:

Trizma-base	30 g
Glycine	144 g
Distilled water	1000 ml

Diluted in 20% methanol to 1 x transfer buffer for immunoblotting

0.5 M Tris-HCl, pH 6.8:

Trizma-HCl	17.5 g
Trizma-base	1.7 g
Distilled water	250 ml

1.5 M Tris-HCl, pH 8.8:

Trizma-HCl	9.2 g
Trizma-base	38.5 g
Distilled water	250 ml

10 x TBS (washing buffer):

Trizma-base	12 g
Sodium chloride	80 g
Tween 20	10 ml
Distilled water	1000 ml
Diluted to 1 x in distilled water	

Dulbeccos PBS, pH 7.4:

Potassium chloride	0.2 g
KH ₂ PO ₄	0.2 g
Sodium chloride	8 g
Na ₂ HPO ₄	1.15 g

Solutions for ELISA:**Blocking solution (Invitrogen, Life technologies):**

BSA	5 g
Dulbeccos PBS	1000 ml

Diluent buffer (Invitrogen, Life technologies):

BSA	5 g
Tween 20	1 ml
Dulbeccos PBS	1000 ml

Blocking/diluent buffer (R&D systems):

BSA	10 g
Dulbeccos PBS	1000 ml

Citrate buffer:

Sodium acetate trihydrate	3 g
Distilled water	200 ml

pH 5.5 are adjusted to citric acid.

TMB:

Citrate buffer	11 ml
TMB 6 mg/ml	200 μ l
H ₂ O ₂ (30%)	2.2 μ l

Stop solution:

H ₂ SO ₄	50 ml
Distilled water	1000 ml

Appendix 3: Particle characterization of 100 µg/ml Si10, Si12 and Si50 in water

The intensity and number distribution of particle sizes with respective measured values:



SiNP	Z-Average (diameter)	Poly-dispersity index (PDI)	Peak 1 (diameter, % peak intensity)	Peak 2 (diameter, % peak intensity)	Peak 3 (diameter, % peak intensity)
Si10 100 µg/ml in water	25,18 nm	0,312	30.41 ± 6 nm 76,8%	9.6 ± 1.2 nm 18,3%	732.6 ± 128 nm 4,9%
Si12 100 µg/ml in water	209.4 nm	0.168	233.8 ± 86 nm 100%	-	-
Si50 100 µg/ml in water	54.55 nm	0.079	58.53 ± 14 nm 100%	-	-